

# Character analysis and descriptions of Eocene sphodrine fossils (Coleoptera, Carabidae) using light microscopy, micro-CT scanning, and 3D imaging

Joachim Schmidt<sup>1</sup>, Stephan Scholz<sup>1</sup>, Kipling Will<sup>2</sup>

<sup>1</sup> University of Rostock, Institute of Biosciences, General and Systematic Zoology, Universitätsplatz 2, 18055 Rostock, German

<sup>2</sup> Essig Museum of Entomology, 1101 Valley Life Sciences Building, #4780 University of California, Berkeley, CA 94720-4780, USA

<http://zoobank.org/02E8488B-DDA7-464C-ABC2-39424200939E>

Corresponding author: Joachim Schmidt (schmidt@agonum.de)

Academic editor: Sonja Wedmann ♦ Received 29 December 2021 ♦ Accepted 2 February 2022 ♦ Published 9 February 2022

## Abstract

Of the 12 specimens of *Calathus*-like sphodrine beetles presently known from Baltic and Rovno amber deposits, 11 specimens were investigated using light microscopy, micro-CT scanning, and 3D imaging techniques. For the first time, many significant diagnostic characters of the external morphology and male and female genitalia of Eocene Sphodrini were studied in detail. Based on these data, three fossil species are diagnosed and placed in a natural group characterized by a derived pattern in elytral chaetotaxy and microsculpture and therefore the genus *Quasicalathus* Schmidt & Will, gen. nov. is described to comprise these species. Due to the presence of a styloid right paramere, *Quasicalathus* gen. nov. is considered a member of the sphodrine “P clade” of Ruiz et al. (2009). However, given the absence of synapomorphies of any species group of the P clade, the systematic position of *Quasicalathus* gen. nov. within this clade remains unresolved. The Baltic amber species *Calathus elpis* Ortuño & Arillo, 2009 is redescribed based on additional, fossil, non-holotype material and transferred to *Quasicalathus* gen. nov. Identification of the additional *C. elpis* fossil material remains slightly uncertain due to the non-availability of the holotype for direct comparison coupled with doubts regarding the accuracy of certain character states presented in its original description. Two species are newly described: *Quasicalathus agonicollis* Schmidt & Will, sp. nov., from Baltic amber, and *Q. conservans* Schmidt & Will, sp. nov., from Rovno amber.

## Key Words

Baltic amber, micro-computed tomography, paleoentomology, Rovno amber, systematics, taxonomy

## Introduction

Beetles of the tribe Sphodrini Laporte, 1834 are known from Eocene fossil deposits only as species in the genus *Calathus* Bonelli, 1810 of the subtribe Calathina Laporte, 1834. Occurrence of *Calathus* fossils in Eocene Baltic amber (50–35 Ma; Standke 2008) was first noted by Handlirsch (1908), then Klebs (1910), and later listed in several amber catalogues (e.g., Bachofen-Echt 1949, Larsson 1978, Spahr 1981). Ortuño and Arillo (2009) described *Calathus elpis* from

Baltic amber, which stood as the only sphodrine species from the Paleogene.

The subtribe Calathina of the tribe Sphodrini is a moderately diverse carabid beetle group comprising 173 species distributed in the Holarctic region. The bulk of the species (152) occurs in the Palearctic, 21 species in the Nearctic, and additionally at least 31 endemic species are known to have an extralimital distribution in the Ethiopian Highlands (Bousquet 2012, Hovorka 2017a, Schmidt 2018). The majority of Calathina species are currently placed in the genus *Calathus* Bonelli, 1810. However, a molecular



analysis by Ruiz et al. (2010) showed that *Calathus* and Calathina are paraphyletic, but Calathina in the sense of Hovorka (2017a) is now monophyletic given that the North American *Calathus* (*Certocalathus*) *advena* (LeConte, 1846) was transferred from the subtribe Dolichina Brullé, 1834 to Calathina (Schmidt and Will 2020).

The definition of *Calathus* or Calathina by morphology alone was shown to be challenging because no morphological, autapomorphic character state is known to define these taxa (Schmidt and Will 2020). As a consequence, the monophyly of the subtribe Calathina is well supported by molecular data but can only be defined morphologically by a combination of plesiomorphic characters: i) antennae pubescent from fourth antennomere; ii) elytra with at least one or more discal seta on third interval; iii) dorsal surface of tarsi without pubescence or wrinkles; iv) tarsal claws pectinate; v) one of the aedeagal parameres styloid; vi) presence of a well-developed gonocoxal sensory pit (Lindroth 1956, Ball and Nègre 1972, Sciaky and Facchini 1997, Sciaky and Wrase 1998).

The lack of ostensible morphological synapomorphies creates a problem for the systematic treatment of Calathina fossils and is a significant, and often underappreciated issue for the use of fossils in time calibration of phylogenetic analyses (Ruiz et al. 2008, 2012, Ober and Heider 2010). Given this, previously published works covering representatives of the genus *Calathus* in Paleogene fossil deposits need careful reinvestigation.

*Calathus elpis* was placed in the tribe Sphodrini due to presence of pectinate claws in addition to a combination of morphological features characteristic for Platynini-like Harpalinae beetles (Ortuño and Arillo 2009). The authors did not further discuss their decision of placing the fossil into the subtribe Calathina or genus *Calathus*. The authors suggest that “*C. elpis* could be an ancestor of the ‘*C. mollis* group’ due to similarities in body size and overall shape (Ortuño and Arillo 2009: 60). However, as shown by Schmidt and Will (2020) these features are not sufficient for placement of the fossil into the genus *Calathus*, the subgenus *Neocalathus* Ball & Nègre, 1972 [including *C. mollis* (Marsham)], or even as evidence for a placement relative to the subtribes of Sphodrini. As a consequence, given the current state of knowledge, *C. elpis* is best treated as a member of Sphodrini with uncertain position within that tribe.

The limited availability of many morphological features for analysis is a serious problem for the study of fossils. In particular, this applies to features hidden in the internal parts of the body. Genitalia play a critical role for the systematic placement of species and lineages in many groups of ground beetles, e.g., character states v) and vi) mentioned above for Calathina. In addition, amber fossils are often obscured by a milky coating and refracting flow lines that prevent standard, visual investigation of characters. For example, preservation conditions unfavorable for light microscopic study are

present in the holotype specimen of *Calathus elpis* (see Ortuño and Arillo 2009: 57, fig. 1). Micro-CT scanning techniques offer a possible solution for these problems if amber and embedded fossils (or their imprints) show sufficient density contrast (Schmidt et al. 2016, 2019, Schmidt and Michalik 2017).

As discussed above, morphological evidence for relationships among clades of sphodrine fossils is problematic but given that such characters are all that is available for fossil taxa it is necessary to critically assess all possible features even if the result can only be considered a working hypothesis. The present study is therefore intended as a first attempt to deal with these problems while comprehensively reviewing the fossil evidence discernible in Paleogene Sphodrini. This study includes a total of 11 inclusions of *Calathus*-like beetles, each preserved in different pieces of Baltic and Rovno ambers, using both light microscopy and micro-CT scanning techniques. All the fossilized specimens studied share character states in the original description of *C. elpis* by Ortuño and Arillo (2009) and, based on a much more comprehensive set of morphological features developed during this investigation, including those from male and female genitalia, the systematic position of *C. elpis* is reviewed. The morphological variability of all the Eocene sphodrine species is reviewed, and two additional species are described.

While in most regards the study is comprehensive and based on first-hand observations, our study is not definitive in some points because important issues related to species-specific taxonomy and morphology cannot be resolved at this juncture. The primary limiting factor was the lack of access to the holotype specimen of *C. elpis*, for reasons we were unable to ascertain (see section Material and Methods). Therefore, this study also stands to point out the consequences when nomenclaturally relevant material is not made available by scientific institutions or private collectors for reinvestigation by subsequent researchers in an appropriate manner.

## Materials and methods

### Investigated material

Type material: The holotype of *Calathus elpis* Ortuño & Arillo, 2009 could not be studied. Based on the original description, the type with collection number MCNA-13638 should be deposited in the Álava Museum of Natural Sciences (Vitoria, Spain) (Ortuño and Arillo 2009: 56). Between 2016 and 2020 email messages sent to the museum address found online at various sources (e.g., <https://www.gbif.org/publisher/4c91866b-3c2e-4568-aca0-3ab-0a1c1a45e>) and emails sent to the authors of the fossil *Calathus* species remained unanswered. Multiple attempts to make contact by telephone using the number



**Table 1.** Micro-CT scan settings.

	<i>Quasicalathus elpis</i>							<i>Q. agonicollis</i>			<i>Q. conservans</i>		
	Groehn 4879	Groehn 7814	Groehn 7889	Abdomen	Groehn 7962	CCHH 952	OSAC 265	MAIG 76	GZG 16185	Holotype SDEI 2528	GZG 16188	Abdomen	Holotype SDEI 2529
Voltage [V]	40	40	40	40	40	30	50	40	40	50	40	40	50
Power [W]	8	8	8	8	8	5	8	8	8	8	8	8	8
Object lens	4	4	4	4	0.4	0.4	4	0.4	4	4	4	20	4
Lens filter	none	none	none	none	none	LE 1	none	none	none	LE 4	none	none	LE 4
Cam binning	2	2	2	2	2	2	2	2	2	2	2	2	2
Distance to source [mm]	122	100	80	40	40	27	96	37	106	40	110	40	96
Distance to detector [mm]	36	40	50	80	300	177	37	260	21	30	70	9	45
Vertical stitch	2	2	3	none	none	none	2	none	2	3	2	none	2
Voxel size [μm]	5.2	4.77	4.14	2.24	7.84	8.73	4.87	8.3	5.63	3.84	4.15	1.09	4.58
Exposure time [sec]	variable 15–22.5	20	10	18	20	30	20	10	15	10	12	25	24
Number of images/ segment	2201 (360°)	2201 (360°)	2001 (360°)	2301 (360°)	2001 (360°)	2001 (360°)	2001 (360°)	1011 (198°)	2001 (360°)	1321 (188°)	1601 (360°)	2101 (360°)	2001 (360°)

listed at the same internet sources failed to connect with personnel at the museum.

Additional material: Ten *Calathus*-like sphodrine specimens preserved in pieces of Baltic amber and one specimen preserved in Rovno amber were studied. For details of the collection data and the respective preservation state of the fossils see species diagnoses and Acknowledgements below.

Investigation techniques

The fossil specimens were studied and imaged via light microscopy and micro-computed tomography (micro-CT) using the Xradia 410 Versa-X-ray microscope (Zeiss, Pleasanton USA). These methods were described in detail in our previous papers (Schmidt et al. 2019, 2021). Micro-CT scan settings used for 3D imaging of the specimens are shown in Table 1. Volume rendering of image stacks was performed by using Amira 6.1 software (FEI Visualization Science Group, Burlington, USA) using the “Volren”, “Volume Rendering” and “Segmentation” functions.

Measurements and proportions

The measurement software of Amira was used and applied to the X-ray scanning results of the fossils (Table 2). The length of the head was measured from anterior margin of clypeus to a point on the midline at the level of the posterior margin of the compound eye. The width of the head was measured in two ways: first, across the widest portion including the compound eyes [‘head width including eyes’ = HW(+)] and second, across the shortest distance between the eyes [‘head width between eyes’ = HW(-)]. The length of the eye and the length of the third antennomere were measured between their most distant points (for the eye in lateral aspect). Length of the pronotum was measured from apical to basal mar-

gin along the midline. The width of the pronotum and the width of each elytron were measured at their widest points (in dorsal aspect). The width of the pronotal apical margin was measured between the tips of the front angles. The width of the pronotal base was measured between the tips of the hind angles at the level of the laterobasal seta. The elytral humeral width was measured between the tips of the humeral angles. The length of each elytron was measured from the apex of scutellum to the apex of the respective elytron. The length of the metepisternum was measured along the lateral margin, its width along the anterior margin. The length of the femur, the apical gonocoxites and the aedeagal median lobe were measured along their greatest lengths. Measurements are not presented from body parts that were deformed due to gas formation (Fig. 61), and those, that yield insufficient contrast during micro-CT scan.

Body length is given as standardized body length (SBL), which equals the sum of the lengths of the head, pronotum, and the longer elytron.

Ratios were presented as follows:

**A3L/HL**

length of third antennomere to length of head;

**EyL/ HW(-)**

length of eye to head width between eyes;

**PW/HW(+)**

pronotal width to head width including eyes;

**PW/PL**

width to length of pronotum;

**PW/PWb**

width of pronotum to width of pronotal base;

**PWb/PWa**

width of pronotal base to width of pronotal apical margin;

**EW/PW**

width of elytra to width of pronotum;

**EL/EW**

length of the longer elytron to width of elytra;

**EpL/EpW**

length to width of the metepisternum;

**EL/FL**

length of the longer elytron to length of the longer femur;

**EL/AedL**

length of the longer elytron to length of the aedeagal median lobe.



**Table 2.** Measurements [µm].

	<i>Quasicalathus elpis</i>								<i>Q. agonicolis</i>		<i>Q. conservans</i>
	Groehn 4879	Groehn 7814	Groehn 7889	Groehn 7962	CCHH 952	OSAC 265	MAIG 76	GZG 16185	Holotype SDEI 2528	GZG 16188	Holotype SDEI 2529
Head length	933	898	950	n.a.	960	930	1038	1057	730	842	899
Head width including eyes	1440	1407	1427	1441	1380	1427	1524	1584	1258	1260	1392
Head width between eyes	885	822	801	827	848	813	875	888	750	779	779
Eye length (left)	577	587	582	652	560	608	622	676	465	503	560
Eye length (right)	n.a.	573	552	627	550	609	620	677	474	475	570
Antennomere 3 length (left)	406	359	382	404	411	396	429	n.a.	325	367	396
Antennomere 3 length (right)	416	366	n.a.	403	398	n.a.	429	446	n.a.	372	n.a.
Pronotal length	1732	1662	1584	1724	1637	1690	1590	1883	1450	1459	1537
Pronotal width	2238	2090	2053	2183	2110	2120	2111	2510	1824	1837	1952
Pronotal apical width	1328	1223	1283	1299	1275	1282	1377	1473	n.a.	1170	1213
Pronotal basal width	2046	1969	1864	2046	1872	1931	2051	2238	1559	1633	1770
Pronotal basal angle	115°	115°	110°	110°	115°	110°	110°	95°	115°	125°	115°
Elytral humeral width	2101	1988	1992	1926	1962	1998	n.a.	2254	1881	1852	1958
Elytral length (left)	5705	4953	5107	5264	5425	5151	4870	5868	4561	4575	4833
Elytral length (right)	5693	4977	5101	5284	5419	5149	4837	5889	4517	4568	4841
Elytral width (left)	1779	1633	1640	1777	1732	1721	n.a.	1995	1483	1465	1610
Elytral width (right)	1745	1569	1690	1706	1731	1682	1730	1857	1438	1531	1600
Metepisternum length (left)	1152	1060	1014	1110	n.a.	1111	n.a.	n.a.	937	971	1060
Metepisternum width (left)	724	689	637	699	n.a.	723	n.a.	n.a.	671	598	742
Metepisternum length (right)	1116	1035	1016	n.a.	n.a.	1162	1104	n.a.	917	1016	1025
Metepisternum width (right)	717	689	652	n.a.	n.a.	725	750	n.a.	631	639	718
Metafemoral length (left)	2163	1912	n.a.	2069	2004	2034	2042	2436	1886	1814	1874
Metafemoral length (right)	2158	1890	n.a.	2058	2093	2068	2069	n.a.	1865	1772	1880
Apical gonocoxite (left)	n.a.	n.a.	178	n.a.	n.a.	n.a.	n.a.	n.a.	n.a.	150	n.a.
Apical gonocoxite (right)	n.a.	n.a.	179	n.a.	n.a.	n.a.	n.a.	n.a.	n.a.	154	n.a.
Aedeagus length	n.a.	1230	n.a.	n.a.	n.a.	n.a.	n.a.	n.a.	1120	n.a.	1331

Description of male genitalia

Herein we use the orientation terms (left and right lateral, dorsal, ventral) for male genitalia that are homologous across Coleoptera and not with respect to the orientation found in Carabidae that is the result of torsion when genitalia are retracted within the apex of the abdomen.

Results

Taxonomic chapter

**Genus *Quasicalathus* Schmidt & Will, gen. nov.**  
<http://zoobank.org/389A05CE-C2C1-4C31-9E8D-F0F9C1CBC1FD>

**Type species.** *Quasicalathus conservans* Schmidt & Will, sp. nov., fossil species from the Eocene Rovno amber, herein designated.

**Species included.** Three fossil species from Eocene amber deposits of Central Europe:

*Quasicalathus agonicolis* Schmidt & Will, sp. nov. (Baltic amber).

*Quasicalathus conservans* Schmidt & Will, sp. nov. (Rovno amber).

*Quasicalathus elpis* (Ortuño & Arillo, 2009), new combination (Baltic amber).

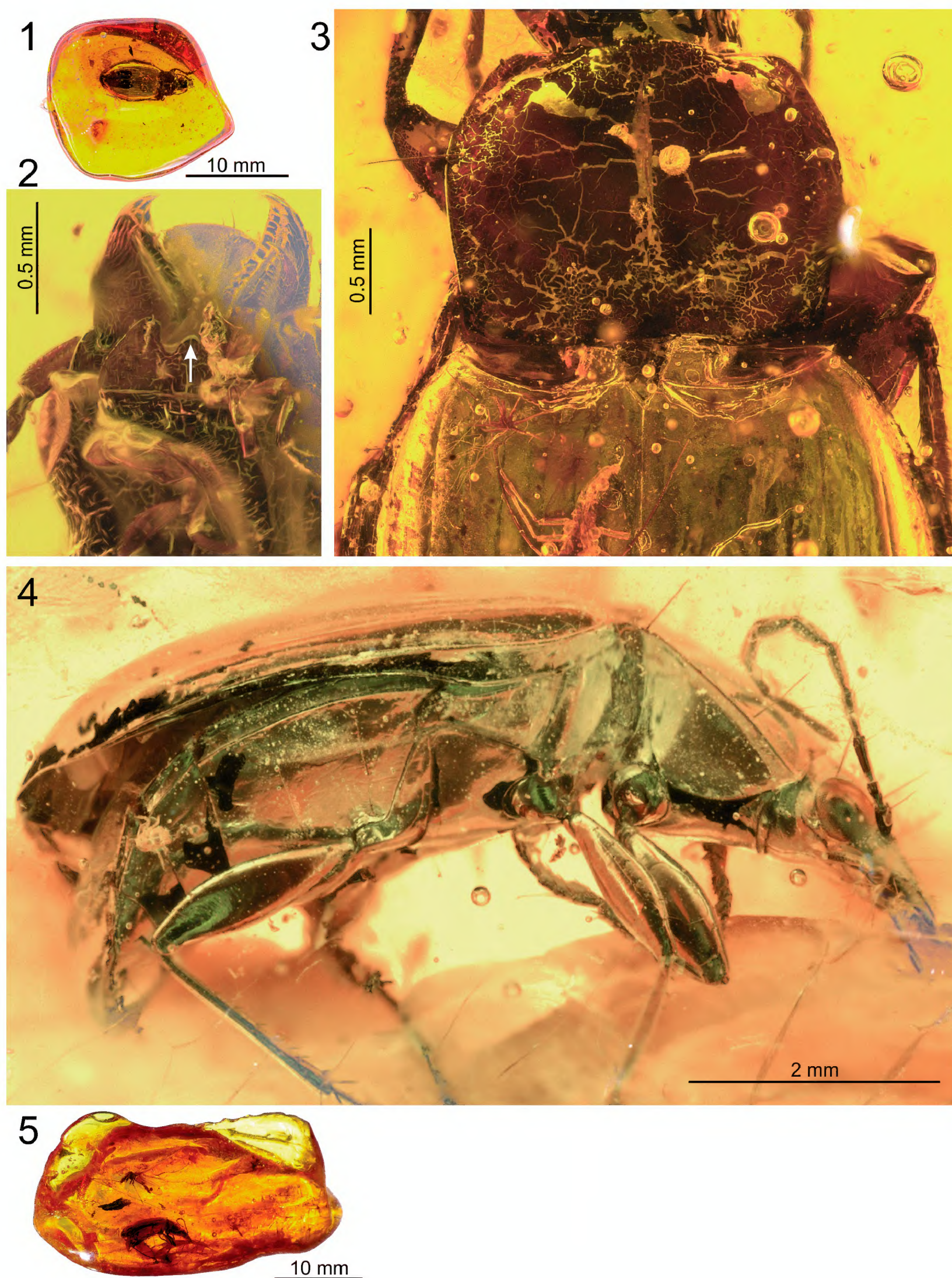
**Diagnostic characters.** Taxon with characteristics of Calathina and *Calathus*, respectively, as defined by Lindroth (1956) and Ball and Negre (1972). The combination of the following character states defines the group:

Head: normal for Calathina, not thickened (Figs 24, 41, 81); mandibles normal for Calathina, not broadened, not elongated (Figs 2, 52); eye size averaged for Calathina, normally protruded (Figs 24, 41); antennae pubescent from fourth antennomere (Fig. 20); mentum tooth simple or slightly truncated at tip, with two fine setae near its base (Figs 52, 82); submentum with two setae each side in normal position, with the internal setae robust and the external setae markedly short and thin (Figs 31, 52, 84).

Prothorax: pronotal shape subquadrate (“calathoid” form; Figs 3, 14, 34, 42, 50, 58–60, 63, 64, 73, 78), slightly or moderately constricted toward base, with lateral margin straight or slightly concave before base, and with basolateral angles slightly or moderately obtuse (Figs 9, 14, 25, 42, 50, 63, 64, 74, 78); basolateral angles not protruded posteriorly; basal margin beaded laterally (level of basolateral angles); basolateral seta situated at margin (Figs 9, 14, 20, 25, 42, 50, 66, 74); pronotal disc with sculpticells of microsculpture transverse, very narrow (magnification 80×). Prosternum impunctate, smooth, prosternal process with or without apical bead (Figs 37, 38, 51, 75, 85).

Pterothorax: elytra slender, ovate, glabrous, humeral tooth absent; basal bead moderately or markedly concave with humeral angle +/- markedly protruded anteriorly (Figs 9, 14, 25, 34, 47, 58–61, 66, 74, 78); epipleuron without plica (Fig. 53); striae slightly to moderately deeply engraved, with punctures evident (Figs 25, 27, 58); intervals flat to moderately convex; parascutellar seta present (Figs 14, 66, 74); third interval with a single rather short, thin discal seta situated near the end of the apical elytral 2/3, adjoining second stria (Figs 11, 12, 16, 27, 29;



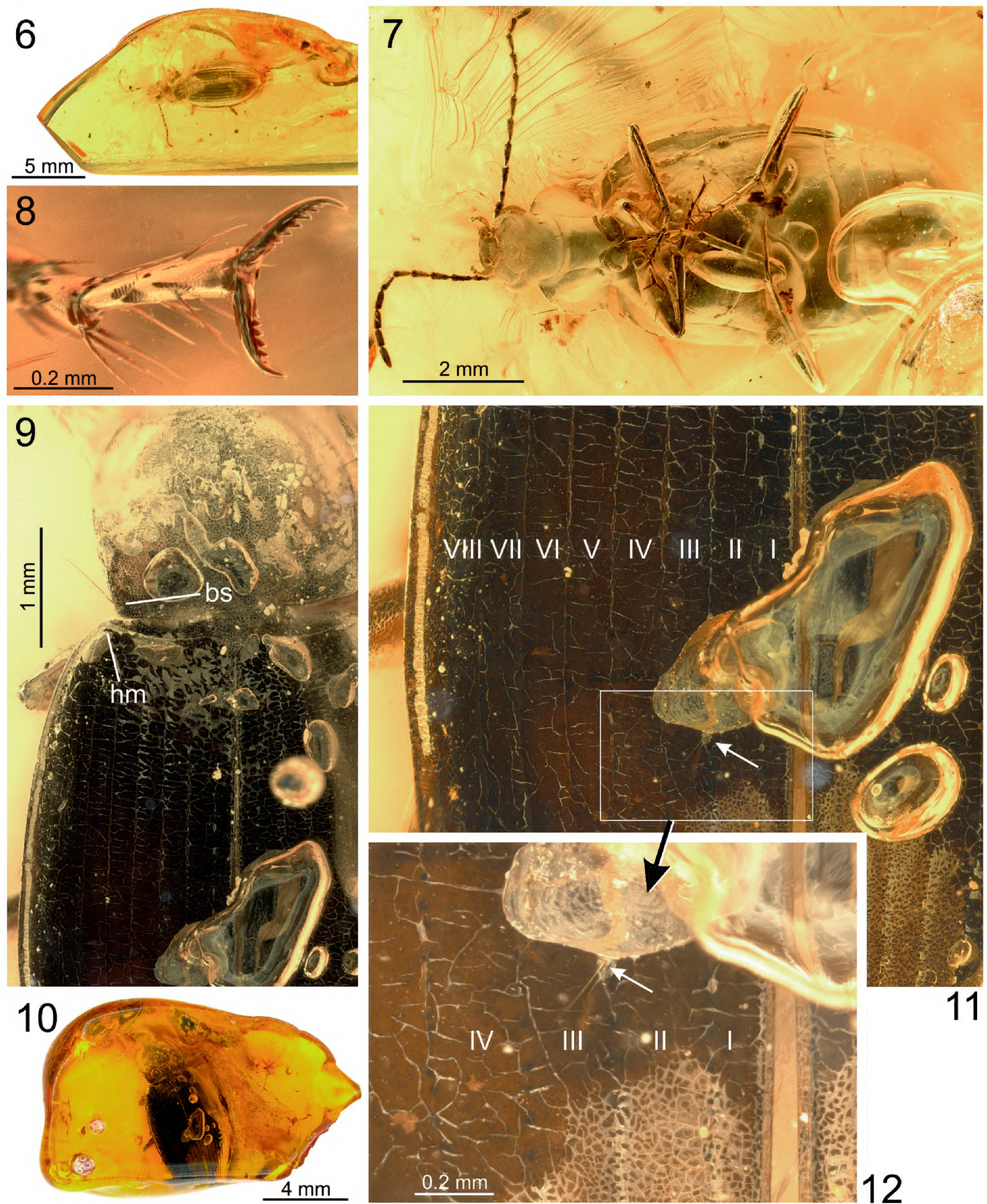


**Figures 1–5.** *Quasicalathus elpis* (Ortuño and Arillo 2009), light microscopic images of specimens “Groehn 4879” (1–3.) and “Groehn 7814” (4, 5.). **1, 5.** General view of the amber pieces; **2.** Ventral side of head (the white arrow points to the mentum tooth; note that the mentum is somewhat detached from the head capsule); **3.** Pronotum and anterior part of elytra showing the markedly concave basal margin and projected humeri; **4.** Right lateral view of body.

but see comments to the redescription of *Q. elpis*, below), with surroundings of setigerous puncture not depressed; external intervals without setae; intervals with sculpticells of microsculpture transverse, very narrow, narrower than on pronotum (Fig. 26; magnification 100×, elytra appearing polished at 40×). Metepisternum elongate (Figs 4, 62, 83). Hindwings fully developed.

Legs: length average for Calathina, neither markedly slender nor particular robust (Figs 4, 7, 30, 36, 49, 62); male protarsomeres dilated; mesocoxa with a single ridge seta; metacoxa trisetose, with anterior seta large and with the two posterior setae small and thin, one located near external, one near internal margin (Figs 54, 67, 86; but see comments to the redescription of *Q. elpis*



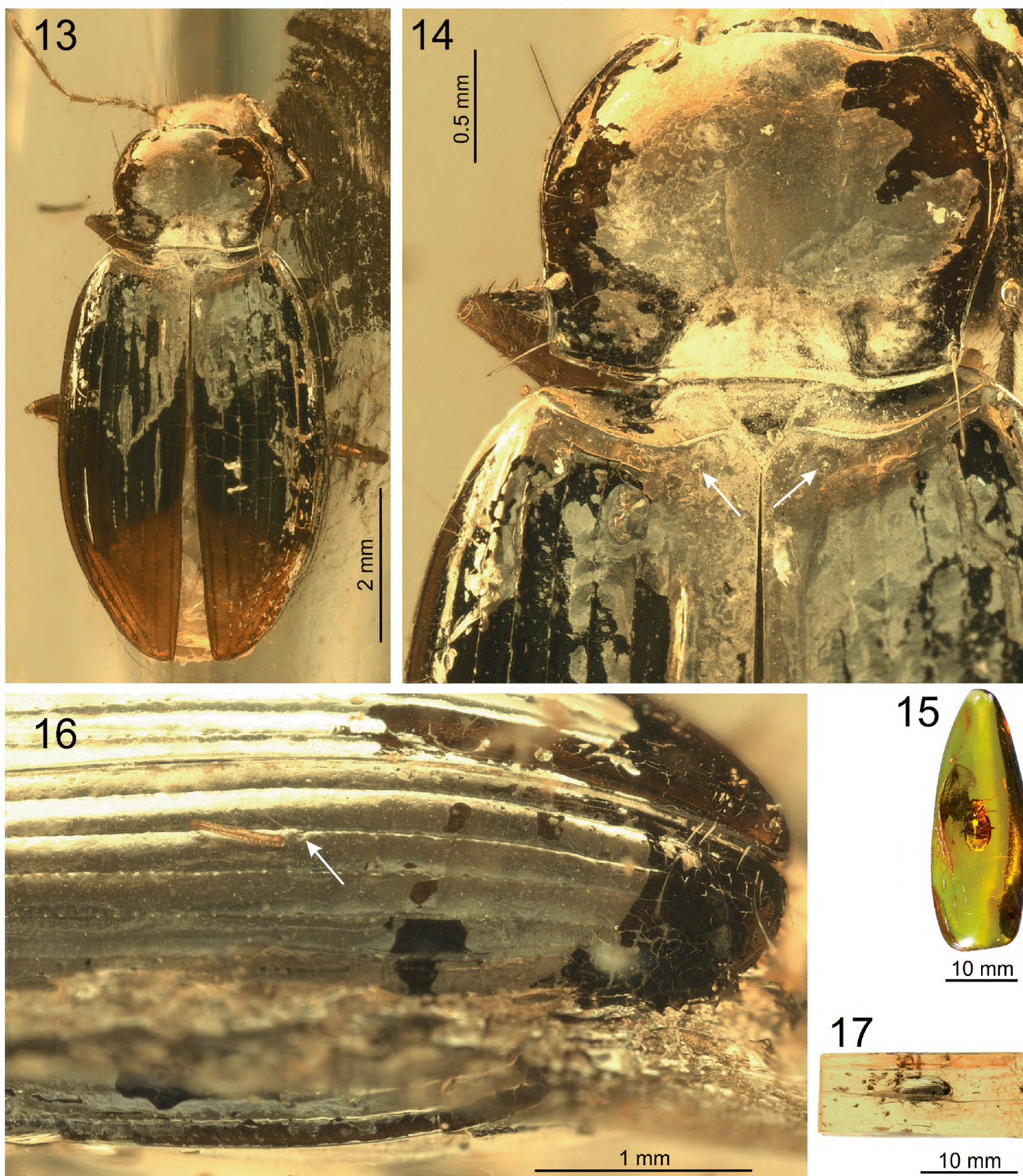


**Figures 6–12.** *Quasicalathus elpis* (Ortuño and Arillo 2009), light microscopic images of specimens “Groehn 7889” (6–8.) and “Groehn 7962” (9–12.). **6, 10.** General view of the amber pieces (in Fig. 6, only the part of the large amber piece bearing the *Quasicalathus* fossil is shown); **7.** Ventral side of body; **8.** Left mesotarsi iv + v; **9.** Pronotum and anterior part of elytra, left side of body; **11, 12.** Medial part of left elytron (Fig. 12 shows the enlarged part of the elytron marked by the white frame in Fig. 11; the white arrow points to the insertion of the discal seta). Abbreviations: **bs** – insertion of the pronotal laterobasal seta; **hm** – humerus; **I–VIII** – elytral intervals 1–8.

below); metatrochanter with seta present (but see comments to the redescription of *Q. elpis*, below); metafemur with two setae on ventral surface, and with dorsoapical

setae present; metatibia in male not densely pubescent; tarsi without pubescence or wrinkles on dorsal surface; meso- and metatarsomeres I–IV without external and in-





**Figures 13–17.** *Quasicalathus elpis* (Ortuño and Arillo 2009), light microscopic images of specimens “CCHH 952” (13–15.) and “OSAC 269” (16, 17.). 13. Dorsal view of body; 14. Pronotum and anterior part of elytra showing the markedly concave basal margin and projected humeri (the white arrows point the insertion pores of the parascutellary setae); 15, 17. General view of the amber pieces; 16. Posterior part of left elytron (the white arrow points to the insertion of the discal seta).

ternal lateral grooves; fifth tarsomeres with a single pair of dorsal setae, and with two pairs of ventral setae; claws pectinate (Fig. 8).

Abdomen: ventrites smooth aside from normal setation; apical ventrite in both sexes with one pair of seta near apical margin (Fig. 53).

Female genitalia (Figs 55–57, 76, 77): basal gonocoxite about two times longer than apical gonocoxite; apical

gonocoxite short, sickle-shaped, with one ensiform seta at dorsal and two ensiform setae at external margin, and with sensory pit large, well-developed, with two setae; basal gonocoxite without setae near apical margin; bursa copulatrix not markedly sclerotized.

Male genitalia (Figs 43–46, 68–72, 80, 87–89): aedeagus right side ventral in repose; right paramere styloid with distal portion very long and slender, not terminat-



ed in a distinct apical hook; left paramere ovoid; median lobe with long apical lamella, without apical disc.

**Etymology.** The name of the new subgenus is derived from the Latin conjunction “quasi” (like; as it were) and the name of the ground beetle genus *Calathus*, and thus refers to the morphological similarity to representatives of this genus.

**Recognition and systematic placement within Sphodrini.** Presence of a styloid right paramere (an apomorphic character state within Sphodrini) differentiates *Quasicalathus* gen. nov. from Atranopsina and Synuchina. Additionally, *Quasicalathus* lacks the stridulation organ that is an autapomorphy for Atranopsina (Casale 1988). Presence of well-developed sensory pit of the apical gonocoxite (plesiomorphic state) differentiates *Quasicalathus* from Synuchina (Casale 1988) and Dolichina sensu Sciaky and Facchini (1997), Sciaky and Wrase (1998) and Hovorka (2017b). Aedeagus with right side ventral in repose (right paramere styloid, left paramere ovoid; plesiomorphic state) differentiates *Quasicalathus* from Pristosiina. The combination of the following characters states places *Quasicalathus* outside of Sphodrina sensu Casale (1988): Mentum tooth not bifid (plesiomorphic state); antennae pubescent from fourth antennomere (plesiomorphic state); tarsomeres without pubescence and smooth on dorsal surfaces (plesiomorphic state); claws pectinate (symplesiomorph with Sphodrini except Atranopsina, reversed in some Sphodrini); aedeagal median lobe slender with long terminal lamella. The shape of the aedeagal median lobe and its terminal lamella is rather variable within Calathina, Dolichina and Synuchina (Lindroth 1956, Habu 1978, Casale 1988).

Based on the overall similarity in external and genital characters the new, fossil genus *Quasicalathus* strongly resembles extant species of subtribe Calathina and genus *Calathus* (see next section). However, as it was comprehensively discussed by Schmidt and Will (2020), monophyly of Calathina is supported by molecular data (Ruiz et al. 2009, 2010) while *Calathus* seems to be paraphyletic, and morphological data supporting Calathina monophyly are currently unknown. As a consequence, the definite, evidence-based, placement of fossil *Quasicalathus* species in this subtribe is currently impossible. What can be stated regarding the systematic placement of this taxon is the following:

- i. *Quasicalathus* is included in the “P clade” of Ruiz et al. (2009) based on the shared presence of the markedly styloid right paramere, which is most likely an autapomorphy of this clade. Atranopsina and all but one outgroup, Zabrinini, are characterized by much shorter parameres. The styloid right paramere shows a pattern of homoplasy across carabids and is considered a separate transformation in Zabrinini as this group has not been shown to be the sister group to Sphodrini in relevant phylogenetic analyses (Ruiz et al. 2009, Gomez et al. 2016).
- ii. *Quasicalathus* is not a member of Synuchina, Dolichina or Pristosiina, as each of these sphodrine sub-

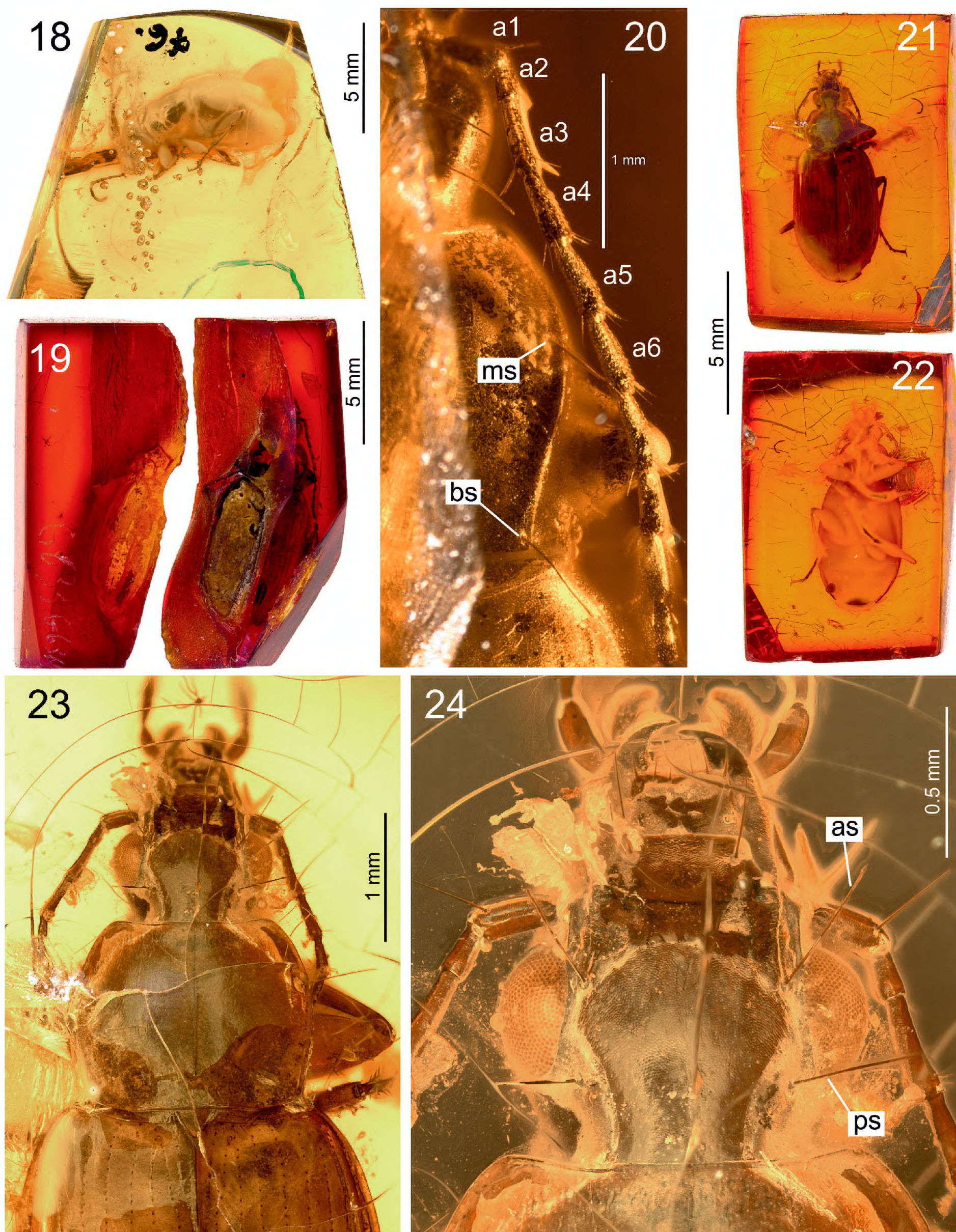
tribes is characterized by respective autapomorphic states that are not present in the fossil specimens.

- iii. *Quasicalathus* is not a member of Sphodrini sensu Casale (1988) because each of the genera affiliated to this subtribe is characterized by at least one autapomorphic state that is not present in *Quasicalathus* (see above).
- iv. Given the lack of apparent morphological synapomorphies for subtribe Calathina and the genus *Calathus* there is currently no evidence that places *Quasicalathus* within, or as sister of, any one of these clades.

Fossils are basic for understanding the evolutionary history of species groups and fossil specimens are critical for time calibration of phylogenetic hypotheses. Therefore, in order to prevent misleading interpretations—e.g., the incorrect assignment of fossils that lack evidence of their placement—we propose the systematic position of *Quasicalathus* using a conservative, synapomorphy-based approach. This requires establishing the genus without a certain position within the sphodrine “P clade” of Ruiz et al. (2009), i.e., Sphodrini, informal group P clade, *incertae sedis*.

**Recognition with respect to Calathina.** The overall similarity of *Quasicalathus* gen. n. with species of the genus *Calathus* makes it necessary to provide a detailed differential diagnosis of the new genus. Recently, Schmidt and Will (2020) presented an overview to the diagnostic characters of the currently accepted genera and subgenera placed within Calathina, and respectively *Calathus*, sensu Hovorka (2017a). The Eocene *Quasicalathus* differs from all calathine species groups by presence of a single elytral discal seta (but see Remarks section to the redescription of *Calathus elpis*, below). All but one Calathina are characterized by presence of at least two elytral discal setae, while the elytra of *Tachalus* Ball & Nègre lacks discal setae. *Quasicalathus* additionally differs from all calathine taxa, with the exception of *Bedelinus* Ragusa, by having a simple mentum tooth (entire instead of bifid), and trisetose metacoxa. *Quasicalathus* differs from all but the Himalayan *Spinocalathus* Schmidt by narrow transverse sculpticells of elytral microsculpture (nearly isodiametric in other Calathina). A slightly transverse pattern of elytral microsculpture is developed in some species of *Denticalathus* Schmidt, however, species of this group differ by pubescent third antennomere in addition to other characters mentioned above and below. *Bedelinus* and *Spinocalathus* differ from *Quasicalathus* additionally by removal of the pronotal laterobasal pronotal seta from the lateral margin, plus presence of lateral grooves on metatarsomeres I–IV. *Quasicalathus* differs from *Spinocalathus* by the short metepisternum, and from *Bedelinus* and most *Spinocalathus* by presence of an apical hook on the right paramere. *Quasicalathus* shares meso- and metatarsomeres I–IV without external and internal lateral grooves with *Iberocalathus* Toribio, *Lindrothius* Kurnakov, some species of *Calathus* s. str., *Denticalathus*, and *Neocalathus* Ball & Nègre. However, species of these groups differ by presence of an apical hook on the aedeagal





**Figures 18–24.** *Quasicalathus*, light microscopic images of *Q. elpis* Ortuño & Arillo, 2009 (18–20.) and *Q. agonicollis* sp. nov. (21–24.). 18. General view of the amber piece “MAIG 76” (only that part of the large amber piece bearing the *Quasicalathus* fossil is shown; the fossil is widely covered by milky coating); 19. General view of the two fragments of specimen “GZG 16185”; the left one bears only the negative imprint of the left elytra on the inclusion wall; 20. Right anterior part of body of specimen “GZG 16185” showing part of head, pronotum and humerus; 21, 22. General view of the amber piece “GZG 16188” (21. With fossil in dorsal view; 22. In ventral view); 23. Anterior part of specimen “GZG 16188”; 24. Head of specimen “GZG 16188”. Abbreviations: **a1–a6** – antennomeres 1–6; **as** – anterior supraorbital seta; **bs** – pronotal laterobasal seta; **ms** – pronotal lateral seta; **ps** – posterior supraorbital seta.



right paramere (*Lindrothius*, *Calathus* s. str., *Denticalathus*, *Neocalathus*) and by a markedly sclerotized spermatheca plus presence of a single ensiform seta along the external margin of the apical gonocoxite (*Iberocalathus*).

Here we hypothesize that i) presence of a single elytral discal seta and ii) presence of narrow transverse sculpticells of elytral microsculpture are synapomorphies of *Quasicalathus* gen. n.; the similarly developed pattern of elytral microsculpture in *Spinocalathus* and some *Denticalathus* are hypothesized as homoplasious as these groups share more derived patterns in some morphological features (e.g., bifid mentum tooth, bisetose metacoxa) together with other Calathina groups.

***Quasicalathus elpis* (Ortuño & Arillo, 2009) comb. nov.**

Figs 1–20, 34–64

*Calathus elpis* Ortuño & Arillo, 2009: 56–60.

**Type material.** Not studied; see Material and methods, above.

**Remarks on original description and recognition.**

The original description of the fossil species *C. elpis* is doubtful or confusing with respect to some important diagnostic characters, these are:

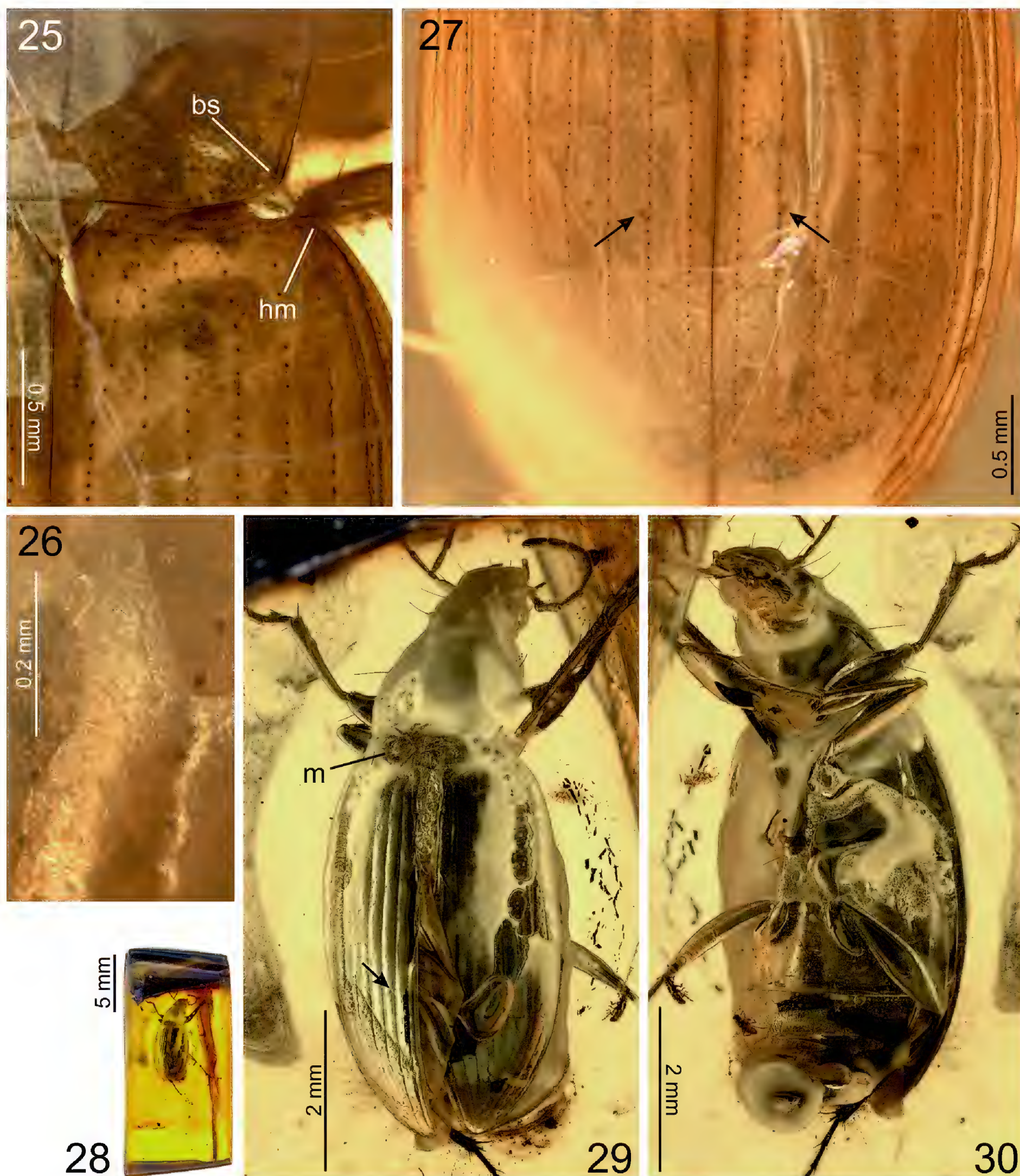
- i. Elytra near middle with two setiferous pores in the 5<sup>th</sup> interval. This pattern of chaetotaxy was not found in any of the fossil species we investigated. In contrast to what was presented by Ortuño and Arillo (2009), we believe that discal setae are absent in the 5<sup>th</sup> interval of the *C. elpis* holotype specimen. It seems likely that the observation of the authors is based on a misinterpretation of micro-structures on the elytral surface of the fossil that are preservation artifacts and thus produce a false impression of existing setiferous pores. This interpretation is supported by the following three facts:  
First, in the reconstruction drawing of the holotype specimen, Ortuño and Arillo (2009: 57, fig. 1d) figured a seta corresponding to each of the reconstructed setiferous pores in the 3<sup>rd</sup> interval (these pores were found in all fossils we studied by us) but do not show those of the external intervals. Therefore, we believe that the authors may have observed structures in the external intervals that appear similar to (but not identical with) setiferous pores but do not bear setae.  
Second, Ortuño and Arillo (2009: 57, fig. 1d) figured pore-like structures in the 6<sup>th</sup> elytral intervals close to the 5<sup>th</sup> striae but not in the 5<sup>th</sup> interval (as reported in their description). Such setation pattern is unknown in sphodrine beetles, fossil or extant. Presence of setiferous pores in the 6<sup>th</sup> elytral interval would also represent a markedly anomalous setation pattern, last but not least because the path of the cubital-1 nerve follows the 5<sup>th</sup> elytral interval (Jeannel 1926).

Third, the character combination ‘3<sup>rd</sup> interval uni-setose + one of the external intervals pluri-setose’ is absent in all other fossil and extant sphodrine species and therefore it is also very likely absent in *C. elpis*.

- ii. Ortuño and Arillo (2009: 58, fig. 2d) presented a reconstruction drawing of the *C. elpis* metacoxa that is bisetose in an irregular way: adjacent to the anterior seta an additional seta on the interior side of the posterior metacoxal surface was figured. Because this setation pattern is unknown in all Sphodrini and other Harpalinae, we believe that it is based on an erroneous interpretation of the actual coxal chaetotaxy of *C. elpis*. Although the majority of sphodrine species are characterized by bisetose metacoxae with one anterior and one posterior seta present, the posterior seta is always located near the external metacoxal margin. Very few Sphodrini possess a trisetose metacoxa with an additional seta interior of the external posterior seta, these include, some Atranopsina, *Bedelinus* of Calathina sensu Hovorka (2017a), *Anchomenidius* Heyden and *Casaleius* Sciaky & Wrase of Dolichina sensu Hovorka (2017b), and all the fossil species from Eocene amber that we investigated. In these extant and fossil taxa, the seta near the internal metacoxal margin is located at the same place as it was figured for *C. elpis* by Ortuño and Arillo (2009: 58, fig. 2d). Therefore, we believe that the external setiferous pore on posterior metacoxal area of *C. elpis* is present but was overlooked by the authors, probably because the seta was broken off or the view obscured, and that the metacoxa of *C. elpis* is actually trisetose as it is in all the other fossil specimens listed in the present study.
- iii. Ortuño and Arillo (2009: 58, fig. 2d) further presented a reconstruction drawing of the *C. elpis* metatrochanter that is asetose. However, the metatrochanters of the holotype specimen actually each are bearing a setiferous pore (Ortuño pers. comm., 2009) as in the diagnosis of *Quasicalathus* gen. n. (see above).

In addition to the doubtful character states discussed above, the original description of *C. elpis* provides few indications that lead to recognition of specimens of this species without direct comparison to the holotype. The ten sphodrine specimens from Baltic amber available for us to study, belong to at least two different species of *Quasicalathus*, and all but one of the diagnostic characters we found to be relevant for these species are absent in the description presented by Ortuño and Arillo (2009). Our interpretation of *C. elpis* as a member of *Quasicalathus* gen. n. is based on the assumption that elytral and coxal chaetotaxy was misinterpreted by the authors of the species as discussed above and, additionally, on the following morphological features evident in the photographs of the holotype specimen provided by Ortuño and Arillo (2009: figs 1b, c): pronotal lateral margin moderately narrowed toward base, straight before laterobasal angles, with



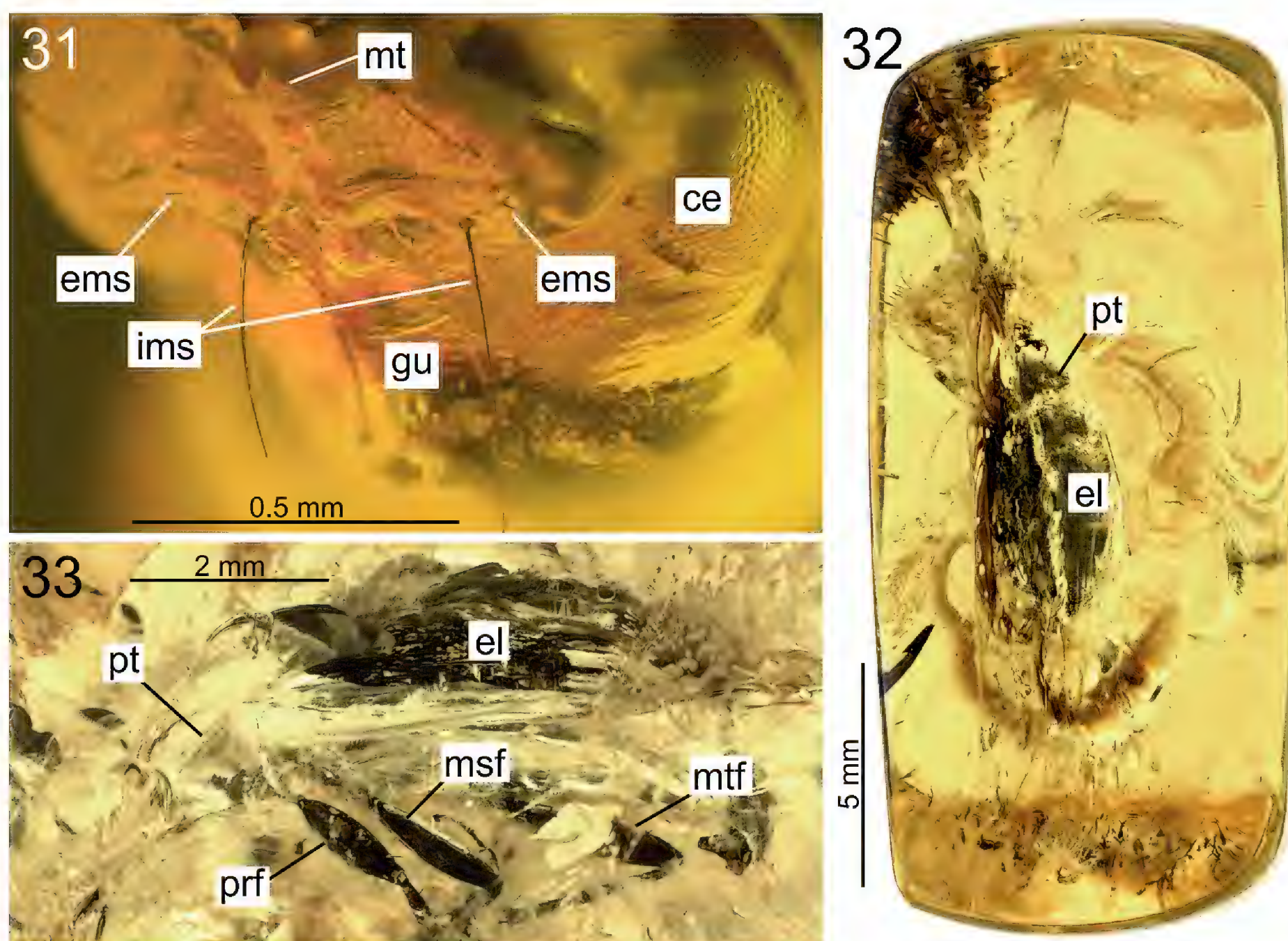


**Figures 25–30.** *Quasicalathus agonicollis* sp. nov., light microscopic images of specimen “GZG 16188” (25–26.) and the holotype (28–30.). 25. Posterior part of pronotum and anterior part of elytra, right side; 26. Anterior part of fifth interval of left elytra showing microsculpture; 27. Posterior part of elytra (the arrows point to the insertions of the discal setae); 28. General view of the amber piece; 29. Right dorsal view of beetle body (the arrow points to the insertion of the discal seta on left elytron); 30. Left ventral view. Abbreviations: **bs** – insertion of the pronotal laterobasal seta; **hm** – humerus; **m** – mite (syninclusion).

the latter moderately obtuse (instead of more rounded pronotal lateral margin with more obtuse laterobasal angles in the Baltic amber fossil species *Q. agonicollis* sp. nov.; see description below). Based on this character, we assume eight of the fossil specimens that are listed under Additional material (below) belong to *C. elpis*.

As a consequence, the redescription of *Quasicalathus elpis* comb. nov. and information about additional morphological characters that we use to distinguish this species from other Eocene sphodrine species (see descriptions of the new fossil species, below) are based on investigation of these eight additional specimens.





**Figures 31–33.** *Quasicalathus*, light microscopic images of the holotypes of *Q. agonicollis* sp. nov. (31.) and *Q. conservans* sp. nov. (32, 33.). 31. Ventral side of head showing chaetotaxy of mentum; 32. General view of the amber piece with fossil in dorsal view; 32. Left lateral view. Abbreviations: **ce** – compound eye; **el** – elytron; **ems** – external seta of submentum; **gu** – gula; **ims** – internal seta of submentum; **msf** – mesofemur; **mt** – mentum; **mtf** – metafemur; **prf** – profemur; **pt** – pronotum.

**Additional material.** Eight specimens, with the following identification numbers, collection data, preservation state, and syninclusions:

**Groehn 4879.** Male in Baltic amber, with specimen label data “Groehn 4879”, deposited in Coll. Carsten Gröhn, Hamburg. Size of the piece approx.  $15 \times 15 \times 4$  mm (Fig. 1).

**Preservation status:** The amber is clear but pervaded by numerous air bubbles; most details of external morphology of the embedded fossil are well visible using light microscope (Figs 2, 3). Some parts of the exoskeleton (head, pronotum, elytral apex) are discoloured black. Using micro-CT, the fossilized beetle body yields moderate to low contrast so that parts of its external shape could only be coarsely imaged (Figs 34–37). The aedeagus is not preserved.

**Syninclusions:** Stellate hairs, additional plant remains, dust particles.

**Groehn 7814.** Male in Baltic amber, with specimen label data “Groehn 7814”, deposited in Coll. Carsten Gröhn, Hamburg. Size of the piece approx.  $35 \times 17 \times 9$  mm (Fig. 5).

**Preservation status:** The amber is pervaded by numerous flowlines and air bubbles and therefore; the embedded fossil is only visible ventrad and right laterad using light microscopy (Fig. 4). The exoskeleton of the fossil is moderately well preserved and important diagnostic characters

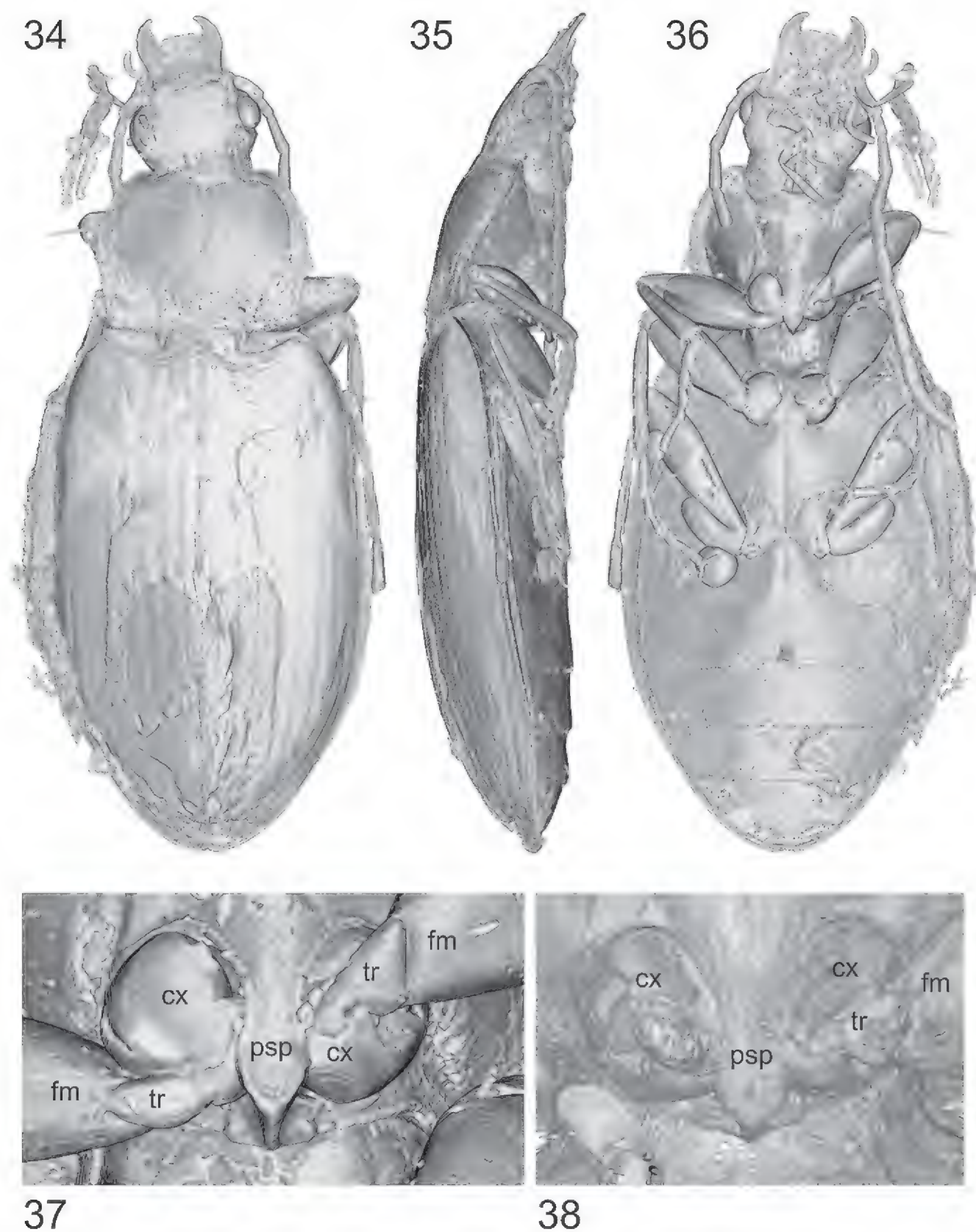
could be imaged using micro-CT (Figs 38, 41, 42). The aedeagus is preserved in most parts (Figs 43–46), however, it was completely detached from the terminal abdominal segments during fossilization of the specimen. Most likely it moved through the abdomen and was finally wedged in the tight connection of meso- and metathorax (Figs 39, 40) after drying out of the internal parts of the beetle.

**Syninclusions:** Stellate hairs, two Nematocera flies, one mite.

**Groehn 7889:** Female in Baltic amber, with specimen label data “Groehn 7889”, deposited in Coll. Carsten Gröhn, Hamburg. The original size of the amber piece was approx.  $35 \times 23 \times 10$  mm and was separated into two pieces (Groehn 7889) in order to get better micro-CT scanning results. The size of the amber piece bearing the calathine fossil measures approx.  $30 \times 11 \times 10$  mm (Fig. 6).

**Preservation status:** The amber is pervaded by an extend flowline attached to the beetle laterally, and a large air bubble is attached to its abdomen ventrally, but most external characters of the beetle are visible using light microscope (Figs 6, 7). The exoskeleton of the fossil is well preserved and could be imaged to show most details using micro-CT (Figs 47–54) including the gonocoxites (Figs 55–57).





**Figures 34–38.** *Quasicalathus elpis* (Ortuño and Arillo 2009), volume rendering of specimens “Groehn 4879” (34–37.) and “Groehn 7814” (38.). 34. Dorsal aspect; 35. Right lateral aspect; 36. Ventral aspect; 37, 38. Prosternum and basal portions of prolegs. Abbreviations: **cx** – procoxa; **fm** – profemur; **psp** – prosternal process; **tr** – protrochanter.

Syninclusions: Plant remains, dust particles.

**Groehn 7962.** Male in Baltic amber, with specimen label data “Groehn 7962”, deposited in Coll. Carsten Gröhn, Hamburg. Size of the amber piece approx.  $14 \times 10 \times 6$  mm, irregularly cut and polished (Fig. 10).

**Preservation status:** The amber is pervaded by numerous flowlines and air bubbles attached to the beetle body, mostly to its ventral surface; the fossil is therefore only partly visible using light microscope (Figs 9–12). Using micro-CT, the fossilized beetle body yields low contrast so that its external shape could only be coarsely imaged (Fig. 58). The aedeagus is not preserved.

**Syninclusions:** None.

**CCHH 952.** Female in Baltic amber, with specimen label data “CCHH#952-2”, deposited in the collection of Christel and Hans Werner Hoffeins, Hamburg. Size of the piece approx.  $39 \times 15 \times 7$  mm (Fig. 15).

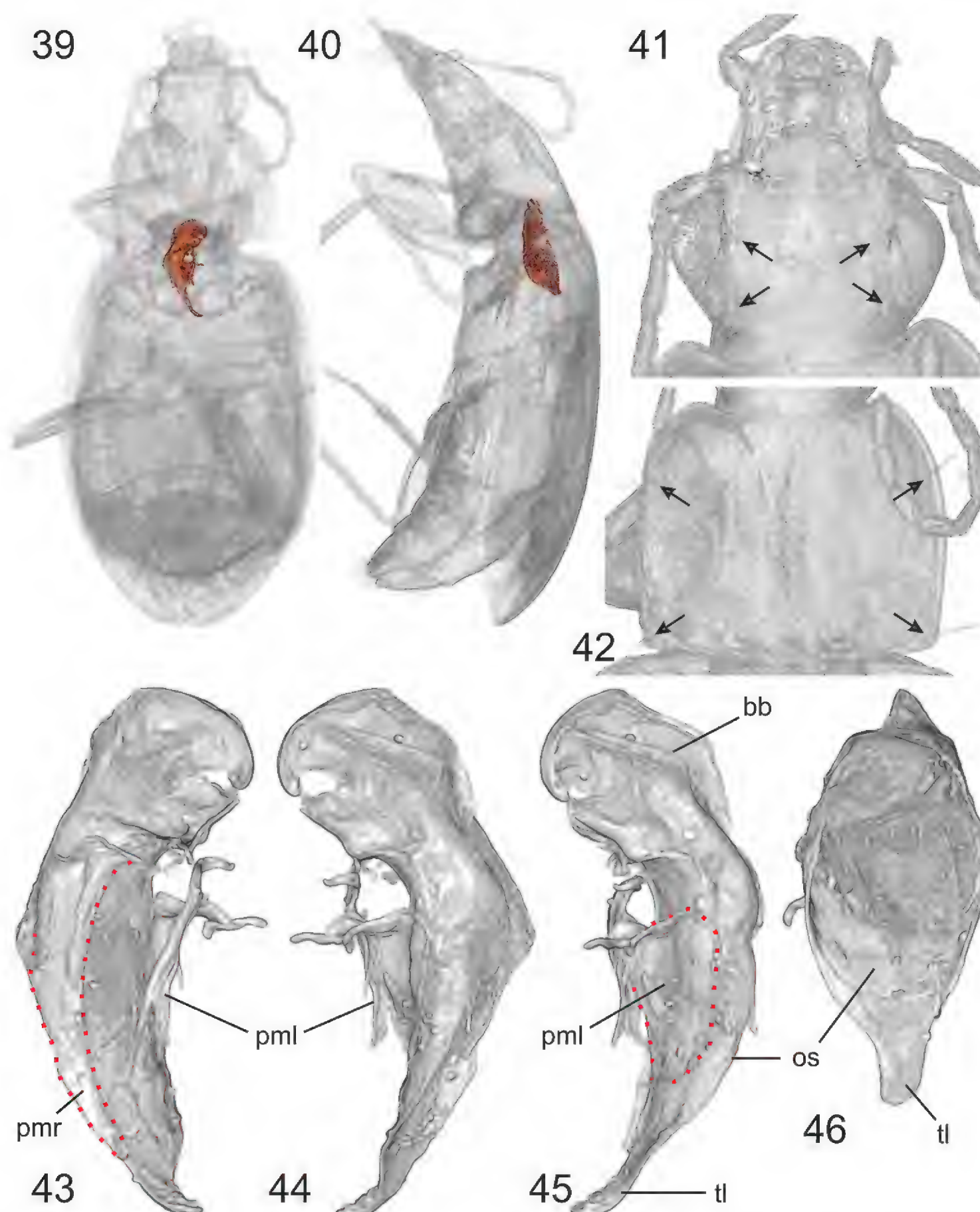
**Preservation status:** The amber is clear in most parts, a single flowline is attached to the right side of the bee-

tle body, which is clearly visible for most of its length using light microscope (Figs 13, 14); head and abdomen are partly covered by a dirty coating ventrally. The amber was likely altered by autoclaving in order to reduce the milky coating. The results of this process are apparent from the blackened appendages of the beetle that are distinctly deformed (particularly tibiae and tarsi), and from one of the synincluded Nematocera that has a roasted appearance. For details on the effect of autoclaving on amber fossils see Hoffeins (2012). Using micro-CT, the fossilized beetle body yields a contrast so that its external shape could only be coarsely imaged (Fig. 59). This is likewise evidence of prior autoclaving of the piece.

**Syninclusions:** Two mites, one Brachycera fly, remains of two Nematocera flies, dust particles.

**OSAC 265.** Male in Baltic amber, with specimen label data “OSAC\_2900265”, deposited in the Oregon State University Collection. The original size of the amber piece was  $57 \times 16 \times 4$  mm and was separated into three





**Figures 39–46.** *Quasicalathus elpis* (Ortuño and Arillo 2009), volume rendering of specimen “Groehn 7814” using different grey scales of the Amira software. **39.** Dorsal aspect; **40.** Lateral aspect. The displaced aedeagus (highlighted by red colour) was separated by the segmentation function of Amira software in Figures 39 and 40; **41.** Head (the arrows point to the insertions of the supra-orbital setae); **42.** Pronotum (the arrows point to the insertions of the lateral setae); **43–46.** Remains of the aedeagus in right lateral aspect (**43.**); Left lateral aspect (**44.**); Left lateral aspect (**45.**); Dorsal aspect (**46.**). The distal margins of the styloid apophysis of the right paramere in Fig. 43 and the lobate apophysis of the left paramere in Fig. 45 are highlighted by red dotted lines. Abbreviations: **bb** – basal bulb of aedeagal median lobe; **os** – distal ostium; **pml** – left paramere; **pmr** – right paramere; **tl** – terminal lamella of median lobe.

pieces in order to get better micro-CT scanning results. The size of the amber piece bearing the calathine fossil measures approx.  $21 \times 9 \times 4$  mm (Fig. 17).

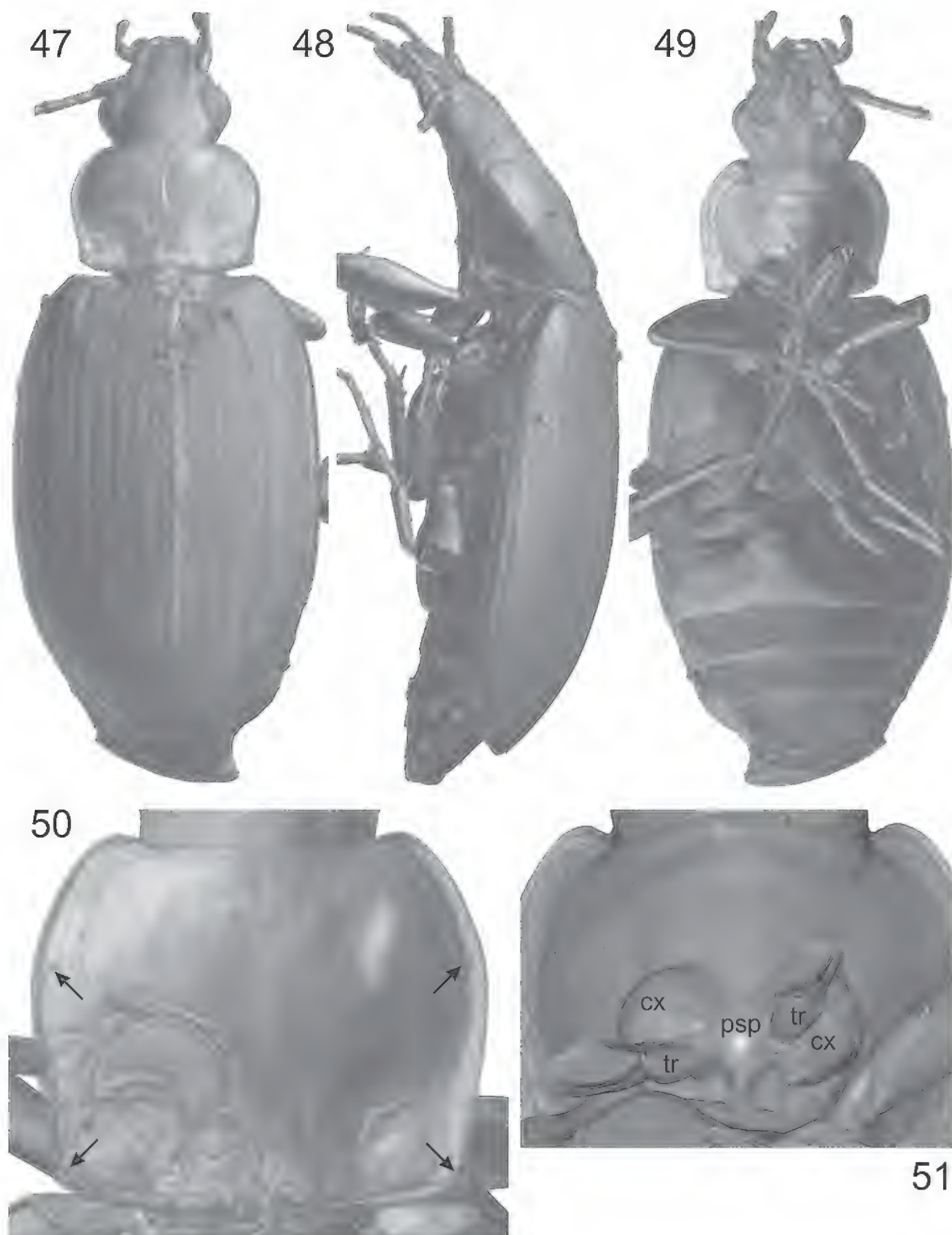
**Preservation status:** The amber is clear in most parts, some flowlines are attached to the embedded fossil; latter is well visible in most parts of the body using light microscope (Figs 16, 17). Using micro-CT, the fossilized beetle body yields low contrast and therefore, its external shape could only be coarsely imaged (Fig. 60). The aedeagus is not preserved.

**Syninclusions:** Large number of dust particles in each of the three pieces.

**MAIG 76.** Female in Baltic amber, with specimen label data “76” deposited in Museum of Amber Inclusions, University of Gdańsk, Poland. Size of the amber piece ca.  $33 \times 23 \times 10$  mm, irregularly cut (Fig. 18).

**Preservation state:** Moderately well preserved due to a large bubble and extensive milky coating attached to the left part of the fossil, resulting in a significant deformation of the beetle body (Fig. 61). A flowline and a corro-





**Figures 47–51.** *Quasicalathus elpis* (Ortuño and Arillo 2009), volume rendering of specimen “Groehn 7889”. **47.** Dorsal aspect; **48.** Left lateral aspect; **49.** Ventral aspect; **50.** Pronotum (the arrows point to the insertions of the lateral setae); **51.** Prosternum (for better view the prolegs are partly removed using the clipping plane function of Amira software. Abbreviations: **cx** – procoxa; **psp** – prosternal process; **tr** – protrochanter.

sion crack are attached to the right side of the beetle body; the apex of the right elytron reaches the amber’s external surface due to a small cavity in the amber piece. Because the fossil yields moderately strong contrast during micro-CT scan, details of its external shape could be imaged apart from the ventral side of the head (Figs 61–63). The genitalic segments are not preserved.

Syninclusions: One tiny insect larva; several air bubbles.

**GZG 16185.** Male in Baltic amber, with specimen label data “GZG BST 16185” and “G633.G636”, deposited in Geoscience Museum, University of Göttingen, Germany (very probably ex coll. Königsberg). Size of the amber piece  $15 \times 8.5 \times 6$  mm, originally with seven polished edges, but fragmented into two pieces of about the same

size, with one piece containing most parts of the fossil while the other contains the negative imprint of the left elytron (Fig. 19); the surface of the latter piece bears the inscription “G633.G636”.

**Preservation state:** Poorly preserved due to amber corrosion; several corrosion cracks pervade the amber surface; amber is markedly darkened with the embedded fossil hardly visible in most views; fossil is partly covered by flowlines, bubbles and milky coating. The fossilized beetle body yields low contrast during micro-CT scan, so that its external shape could only be very coarsely imaged (Fig. 64). The aedeagus is not preserved.

**Syninclusions:** Stellate hairs, dust particles.



**Redescription.** Measurements see Table 2.

SBL: 7.5–8.8 mm ( $\bar{\phi}$  7.9 mm;  $n = 7$ ).

Proportions: A3L/HL = 0.40–0.45 ( $\bar{\phi}$  0.42;  $n = 11$ );

EyL/ HW(-) = 0.65–0.79 ( $\bar{\phi}$  0.72;  $n = 15$ );

PW/HW(+) = 1.39–1.58 ( $\bar{\phi}$  1.50;  $n = 8$ );

PW/PL = 1.26–1.33 ( $\bar{\phi}$  1.29;  $n = 8$ );

PW/PWb = 1.03–1.13 ( $\bar{\phi}$  1.10;  $n = 8$ );

PWb/PWa = 1.47–1.61 ( $\bar{\phi}$  1.52;  $n = 8$ );

EW/PW = 1.53–1.64 ( $\bar{\phi}$  1.29;  $n = 7$ );

EL/EW = 1.51–1.62 ( $\bar{\phi}$  1.55;  $n = 7$ );

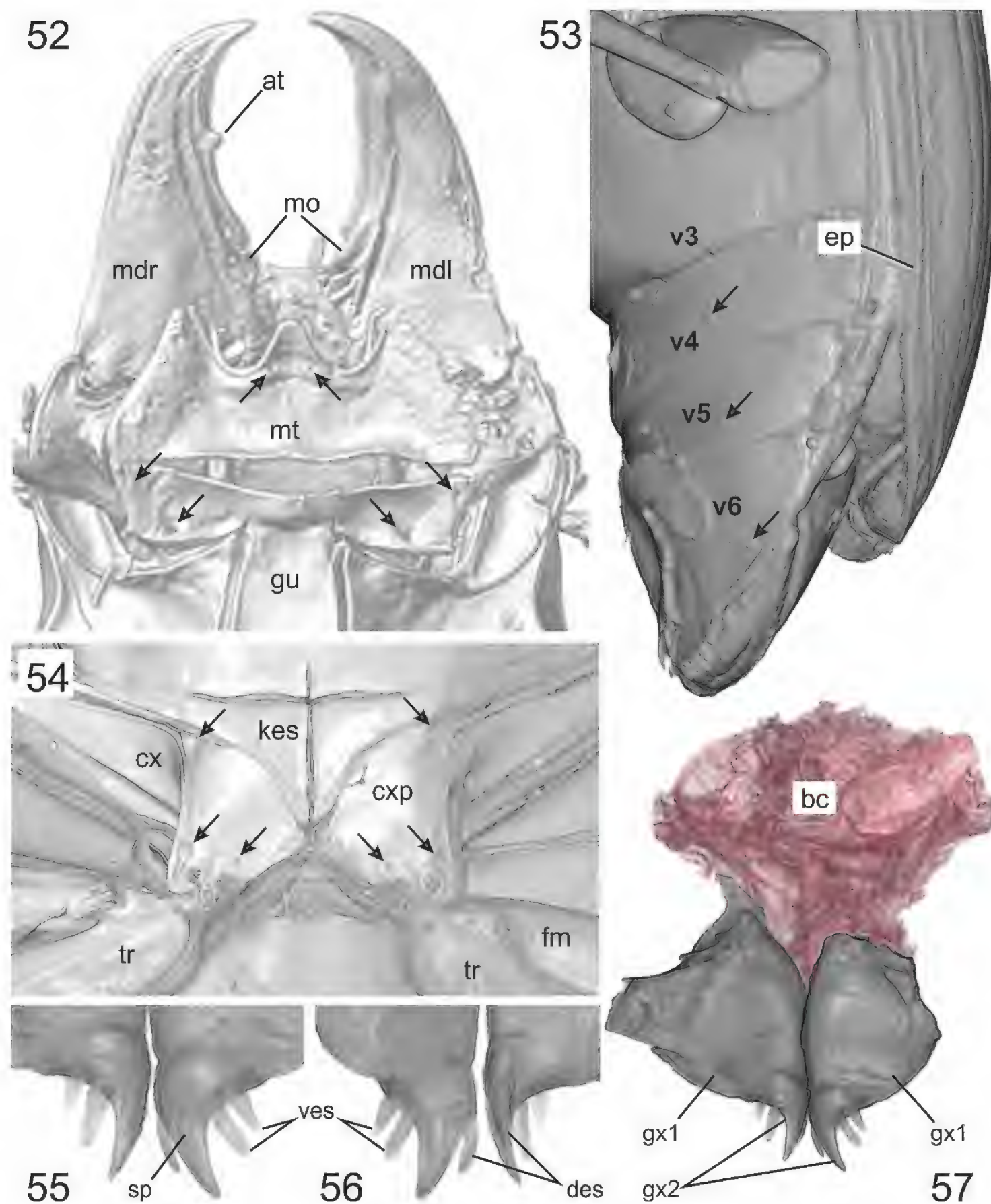
EpL/EpW = 1.47–1.60 ( $\bar{\phi}$  1.55;  $n = 10$ );

EL/FL = 2.35–2.65 ( $\bar{\phi}$  2.53;  $n = 7$ );

EL/AedL = 4.05 ( $n = 1$ ).

Head: Microsculpture on disc consists of very small slightly irregular meshes (magnification 80 $\times$ ). In all other characters as described for the new genus, above.

Prothorax: Pronotal lateral margin moderately narrowed toward base, straight or slightly concave before laterobasal angles, angles slightly obtuse (Figs 3, 9, 14, 34, 42, 50, 58–60, 63, 64). Prosternal process with or without apical bead (Figs 37, 38, 51). In all other characters as described for the new genus, above.



**Figures 52–57.** *Quasicalathus elpis* (Ortuño and Arillo 2009), volume rendering of specimen “Groehn 7889”. **52.** Head, ventral aspect (the arrows point to the insertions of the setae near base of mentum tooth and on submentum); **53.** Abdomen, left lateral aspect (the arrows point to the insertions of the setae on ventrites IV, V, and VI); **54.** Metacoxal area (the arrows point to the insertions of the coxal setae); **55.** Apical gonocoxites, ventral aspect; **56.** Apical gonocoxites, dorsal aspect; **57.** Gonocoxites and remains of the bursa copulatrix (the latter was highlighted by red colour using the segmentation function of Amira software). Abbreviations: **at** – apical tooth of retinacle; **kes** – metathoracic katepisternum; **cx** – metacoxa; **cxp** – metacoxal plate; **des** – dorsal ensiform setae; **ep** – elytral epipleuron; **fm** – metafemur; **gu** – gula; **mdl** – left mandible; **gx1** – basal gonocoxite; **gx2** – apical gonocoxite; **mdr** – right mandible; **mo** – molar; **mt** – mentum; **sp** – sensory pit; **tr** – metatrochanter; **ves** – ventral ensiform setae; **v3, v4, v5, v6** – ventrites III, IV, V, VI.



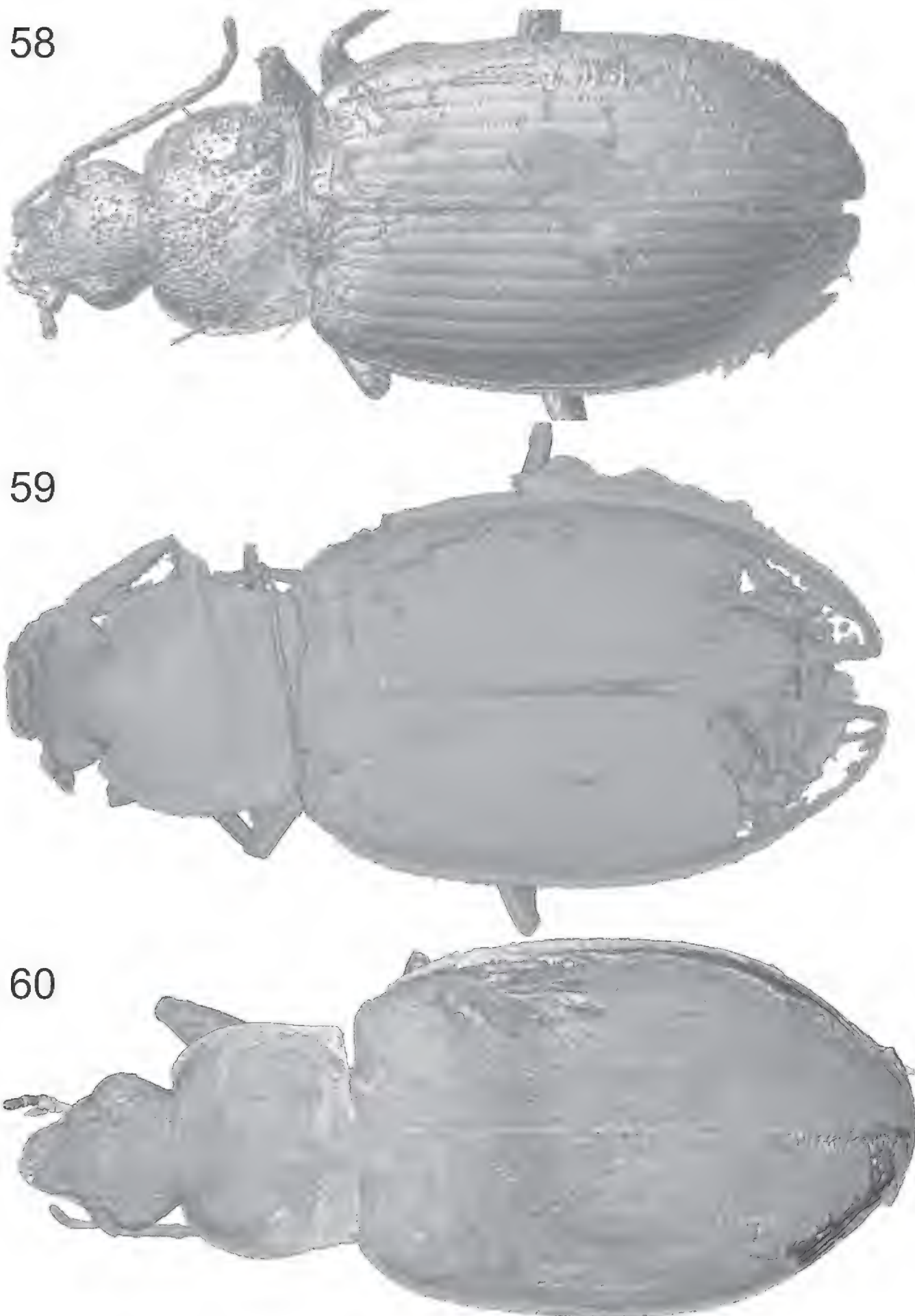
Pterothorax: Elytra with basal margin markedly concave and humerus markedly protruded anteriorly; basal margin forming a slightly obtuse angle ( $100\text{--}115^\circ$ ) with lateral margin (Figs 3, 9, 14, 34, 47, 58–60, 61). Elytral striae moderately deeply engraved, intervals moderately convex. In all other characters as described for the new genus, above.

Female genital: Length of apical gonocoxite about 0.18 mm; shape see Figs 55–57. In all other characters as described for the new genus, above.

Aedeagus: Length of median lobe about 1.23 mm; median lobe terminal lamella moderately long and more markedly narrowed just behind its base so that its left margin is markedly concave and its apex slender lingulate (Fig. 46); in lateral view, terminal lamella markedly bent

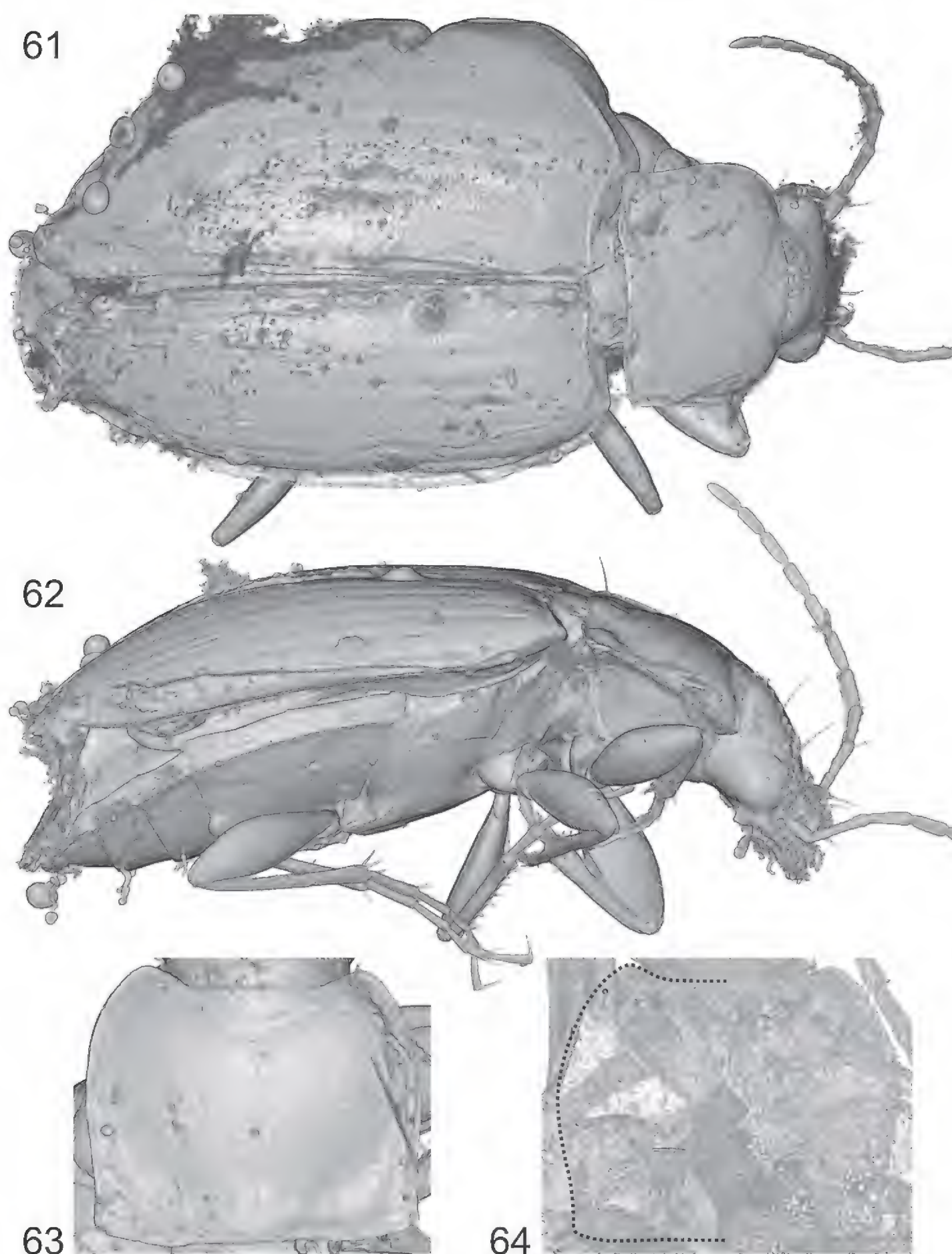
ventrally (Figs 43–45; note that the intensity of ventral bending might also be an artefact of poor preservation). In all other characters as described for the new genus, above.

**Differential diagnosis.** *Quasicalathus elpis* (in sense of this paper) differs from *Q. agonicollis* sp. nov. by larger body (SBL  $> 7$  mm), less obtuse laterobasal angles of pronotum, more concave elytral basal margin, more markedly projected humeri, less obtuse humeral angle ( $< 120^\circ$ ), longer apical gonocoxites and larger aedeagus. It differs from *Q. conservans* sp. nov. by the proportionally smaller aedeagus with terminal lamella bent ventrally (Figs 43–45); the left margin of the terminal lamella in dorsal view is significantly concave in *Q. elpis* (Fig. 46) but almost straight in *Q. conservans* sp. nov. (Fig. 88).



**Figures 58–60.** *Quasicalathus elpis* (Ortuño and Arillo 2009), volume rendering of the dorsal aspects of specimens “Groehn 7962” (58.), “CCHH 952” (59.), and “OSAC 265” (60.).





**Figures 61–64.** *Quasicalathus elpis* (Ortuño and Arillo 2009), volume rendering of specimens “MAIG 76” (61–63.) and “GZG 16185” (64.); 61. Dorsal aspect; 62. Right lateral aspect; 63, 64. Pronotum (the pronotal outline on left side is highlighted by dotted line in Fig. 64).

***Quasicalathus agonicollis* Schmidt & Will, sp. nov.**

<http://zoobank.org/0555D647-EDC0-4A5F-BDDE-05FA1C5BB140>

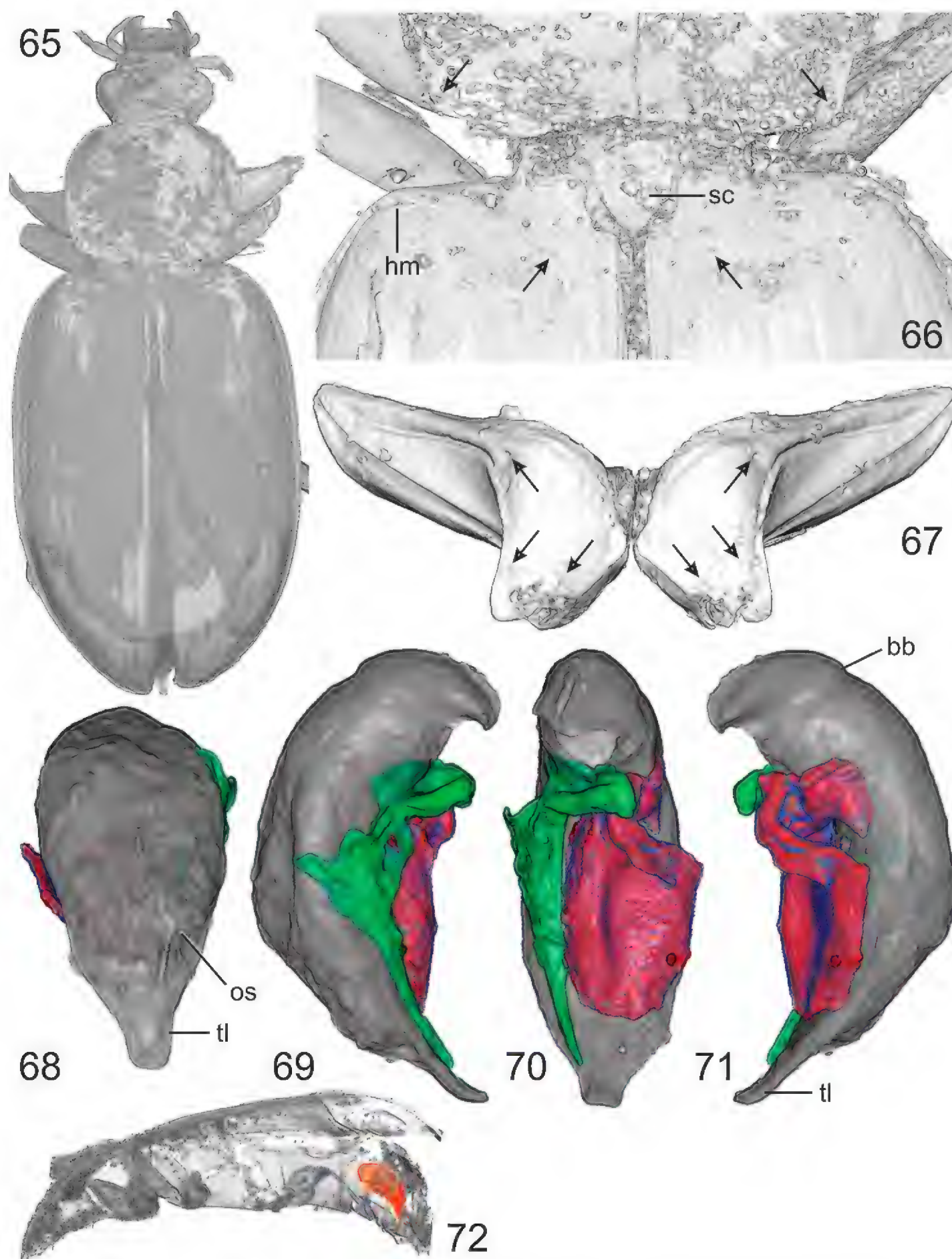
Figs 21–31, 65–77

**Holotype.** Male in Baltic amber, with specimen label data “SDEI-Amb-002528”, deposited in Senckenberg Deutsches Entomologisches Institut, Müncheberg, Germany. The original size of the amber piece was  $60 \times 23 \times 7$  mm and was separated into three pieces (SDEI Amb-002528 a, b, c) in order to get better micro-CT scanning results. The size of the amber piece bearing the calathine fossil measures approx.  $15 \times 9 \times 4$  mm (Fig. 28).

**Preservation status:** A clear piece of amber with the embedded carabid fossil well visible, however, exten-

sive flowlines are present in front of the head and on the right side of the beetle body. Several parts of the beetle body are additionally covered by a white coating so that details of the exoskeleton are not visible using light microscopy; this includes the dorsal surface of head and pronotum, lateral parts of the elytra, right side of the ventral surface (Figs 29, 30). The external surface of the fossilized beetle body yields low (head, thorax) or relatively moderate contrast (elytra, abdomen) during micro-CT scan and therefore, the anterior part of the body could only be coarsely imaged (Fig. 65). The aedeagus with median lobe and right paramere is moderately well preserved and could partly be imaged using micro-CT data (Figs 68–72); the left paramere





**Figures 65–72.** *Quasicalathus agonicollis* sp. nov., volume rendering of the holotype using different grey scales of the Amira software. **65.** Dorsal aspect (the negative imprint of the fossil on the inclusion wall is shown); **66.** Basal portion of pronotum and anterior part of elytra (positive of the fossilized beetle is shown; the arrows point to the insertions of the pronotal basolateral setae and the parascutellar setae); **67.** Metacoxa (the arrows point to the insertions of the three coxal setae each side); **68–71.** Aedeagus in dorsal aspect (**68.**), Right lateral aspect (**69.**), Ventral aspect (**70.**), Left lateral aspect (**71.**); The remains of the parameres are coloured (red: left paramere; green: right paramere); **72.** left lateral aspect of beetle body; the aedeagus (highlighted by red colour) was separated by the segmentation function of Amira software. Abbreviations: **bb** – basal bulb of aedeagal median lobe; **hm** – humerus; **os** – distal ostium of median lobe; **sc** – scutellum; **tl** – terminal lamella of median lobe.

provided contrast during CT scan that was too low for reconstruction.

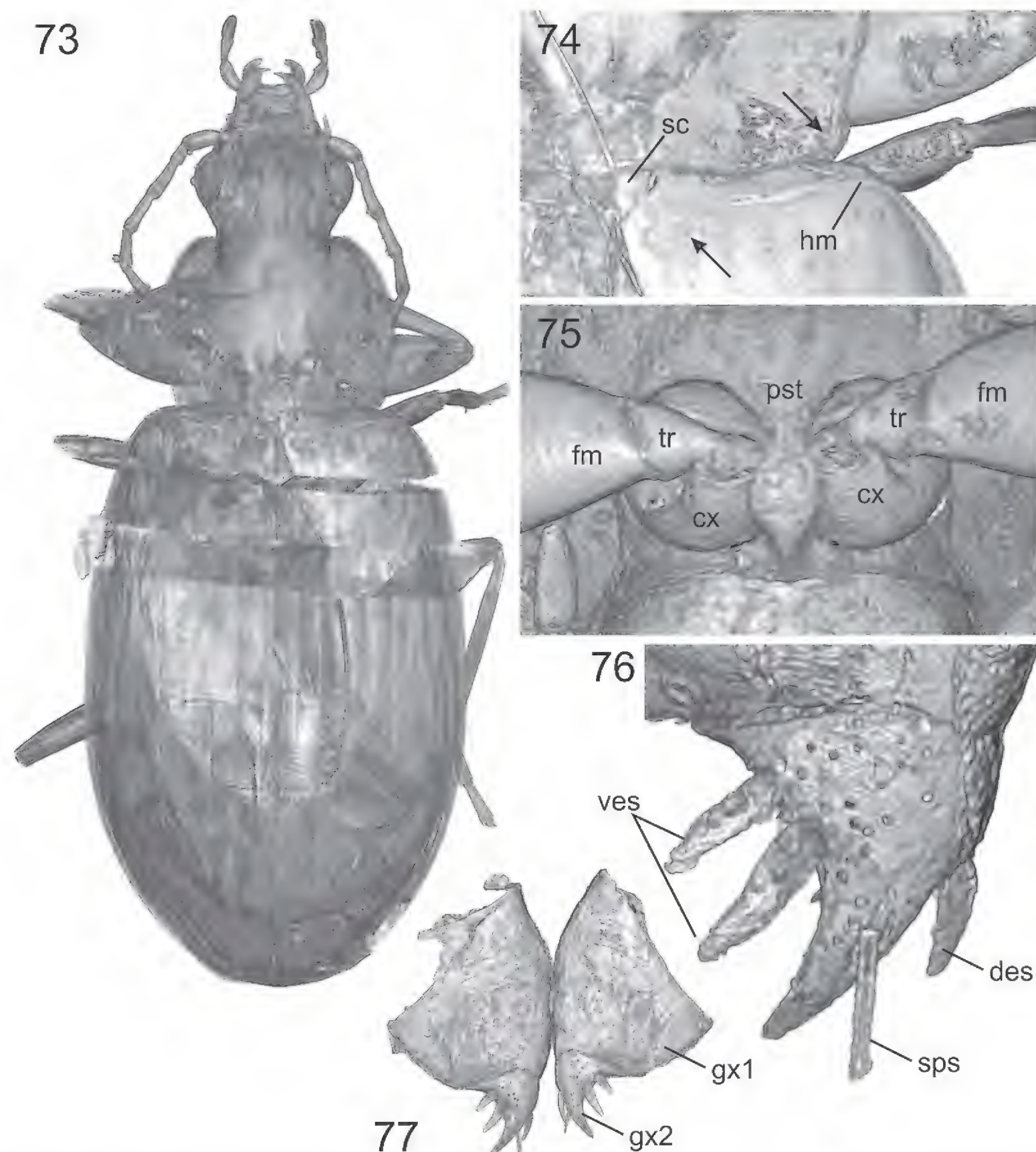
Syninclusions: SDEI-Amb-002528a: seven very tiny insect larva, dust particles; one mite on the carabid fossil near the beetle's scutellum. SDEI-Amb-002528b: one Myrmicinae ant, three Nematocera flies, stellate hairs, dust particles. SDEI-Amb-002528c: dust particles.

**Additional material.** Female in Baltic amber, with specimen label data “GZG BST 16188” and “K2192” (ex

coll. Klebs), deposited in Geoscience Museum, University of Göttingen, Germany. Size of the amber piece approx.  $12 \times 7 \times 4$  mm, with seven polished edges (Figs 21, 22); one edge bears the inscription “G644”.

**Preservation status:** The amber stone is clear in most parts but its surface shows several corrosion cracks (Figs 23, 24); the ventral surface of the fossil is completely covered by a milky coating (Fig. 22). The exoskeleton of the fossil is moderately well preserved and could therefore





**Figures 73–77.** *Quasicalathus agonicollis* sp. nov., volume rendering of specimen ‘GZG 16188’. **73.** Dorsal aspect; **74.** Basal portion of pronotum and anterior part of elytra (right side of body; the arrows point to the insertions of the pronotal basolateral seta and the parascutellar seta); **75.** Prosternum with basal portion of prolegs; **76.** Left apical gonocoxite, ventral aspect; **77.** Gonocoxites, ventral aspect. Abbreviations: **cx** – procoxa; **des** – dorsal ensiform setae; **fm** – profemur; **gx1** – basal gonocoxite; **gx2** – apical gonocoxite; **hm** – humerus; **pst** – prosternum; **sc** – scutellum; **sps** – setae of sensory pit; **tr** – protrochanter; **ves** – ventral ensiform setae.

be imaged in most details using micro-CT (Figs 73–75), including the gonocoxites (Figs 76, 77).

Syninclusions: Stellate hairs, dust particles.

**Remarks.** The specific identity of this second fossil specimen with the holotype of *Q. agonicollis* sp. nov., given the current state is difficult to substantiate. This is due to the poor preservation state of the holotype specimen. In the specimen GZG 16188, the pattern of head microsculpture is quite differently developed from that what we found in *Q. elpis* and the below described *Q. conservans* sp. nov., however, this character state is unknown for the *Q. agonicollis* sp. nov. holotype. Therefore, our decision to identify GZG 16188 as *Q. agonicollis* sp. nov. must be considered provisional. It is based on the following four interspecific diagnostic character states that *Q. agonicollis* sp. nov. holotype

and specimen GZG 16188 share: i) body size small, SBL below 7 mm. ii) pronotal laterobasal angles more markedly obtuse; iii) elytral basal margin moderately concave; iv) humerus slightly protruded with humeral angle more markedly obtuse. Therefore, in the description of *Q. agonicollis* sp. nov. we separate the descriptions of the *Q. agonicollis* sp. nov. holotype and the specimen GZG 16188.

**Description of the holotype.** Measurements see Table 2.

Standardized body length: 6.7 mm.

Proportions: A3L/HL = 0.45;

EyL/ HW(–) = 0.62;

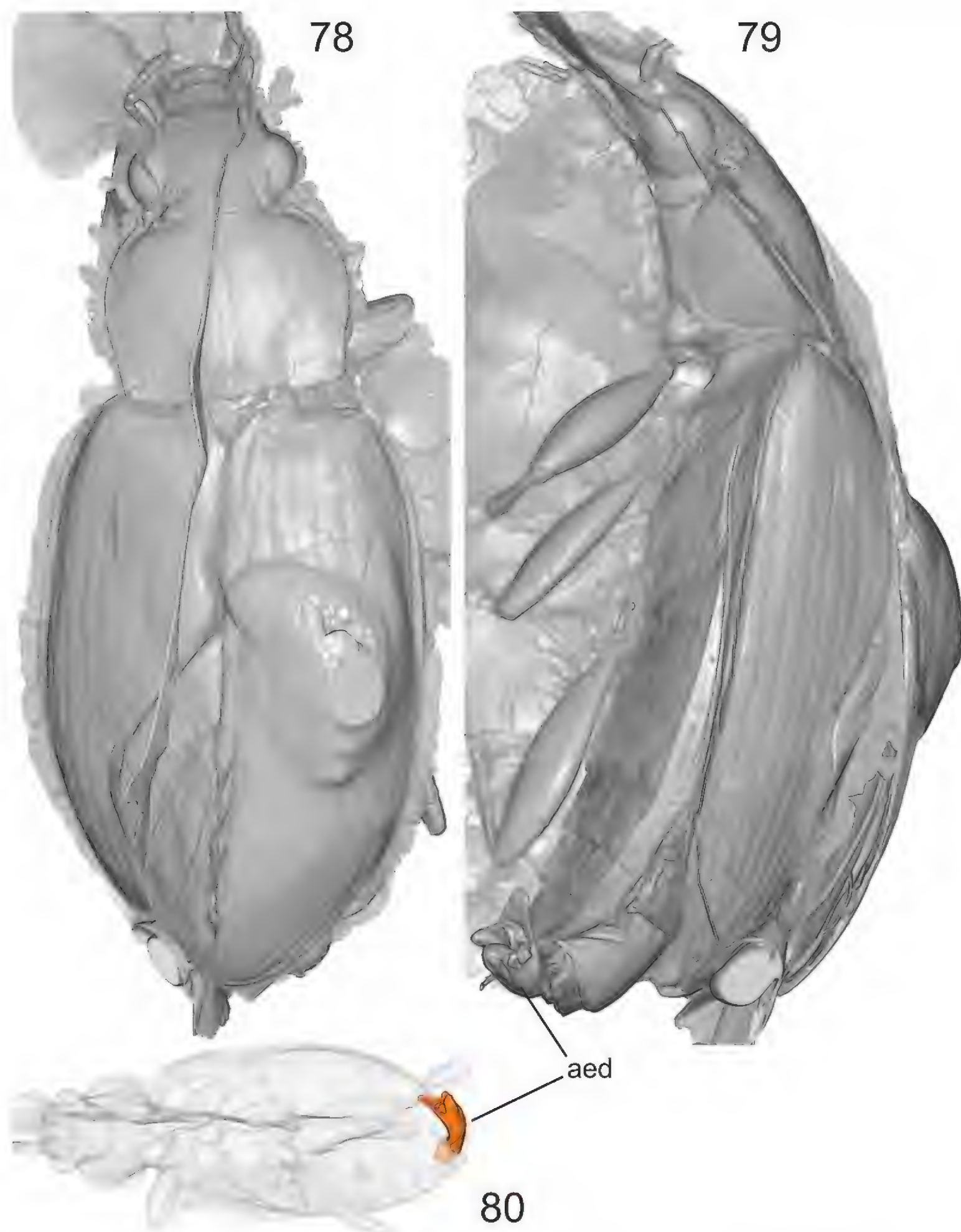
PW/HW(+) = 1.45;

PW/PL = 1.26;

PW/PWb = 1.17;

PWb/PWa = not available;





**Figures 78–80.** *Quasicalathus conservans* sp. nov., volume rendering of the holotype using different grey scales of the Amira software. **78.** Dorsal aspect; **79.** Left lateral aspect (**aed** – aedeagus); **80.** Ventral aspect; the aedeagus (highlighted by red colour) was separated by the segmentation function of Amira software.

EW/PW = 1.60;  
 EL/EW = 1.55;  
 EpL/EpW = 1.40;  
 EL/FL = 2.42;  
 EL/AedL = 4.07.

Head: Patterns of microsculpture could not be studied. In all other characters as described for the new genus, above.

Prothorax: Pronotal lateral margin more markedly narrowed toward base than in *Q. elpis*, straight just before laterobasal angles, angles markedly obtuse (Figs 65, 66). Prosternal process with traces of lateral bead evident. In all other characters as described for the new genus, above.

Pterothorax: Elytra with basal margin moderately concave and humerus moderately protruded anteriorly; basal margin forming a more obtuse angle (ca. 125°) with lateral margin (Figs 65, 66). Elytral striae moderately deeply engraved, intervals moderately convex. In all other characters as described for the new genus, above.

Aedeagus: Length of median lobe 1.12 mm. Median lobe terminal lamella almost evenly narrowed from base to apex with side margins almost straight; apex slightly bent ventrally (Fig. 70). In all other characters as described for the new genus, above.



**Description of specimen GZG 16188.** Measurements see Table 2.

Standardized body length: 6.9 mm.

Proportions:  $A3L/HL = 0.44$ ;

$EyL/HW(-) = 0.65$ ;

$PW/HW(+) = 1.46$ ;

$PW/PL = 1.26$ ;

$PW/PWb = 1.12$ ;

$PWb/PWa = 1.40$ ;

$EW/PW = 1.63$ ;

$EL/EW = 1.53$ ;

$EpL/EpW = 1.62$ ;

$EL/FL = 2.55$ .

Head: Microsculpture consists of moderately large isodiametric sculpticells (Fig. 24). In all other characters as described for the new genus, above.

Prothorax: Pronotal lateral margin almost completely rounded, straight just before laterobasal angles, angles markedly obtuse (Figs 23, 25, 73, 74). Prosternal process with traces of an apical bead (Fig. 75). In all other characters as described for the new genus, above.

Pterothorax: Elytra with basal margin moderately concave and humerus moderately protruded anteriorly; basal margin forming a more obtuse angle (ca.  $125^\circ$ ) with lateral margin (Figs 23, 73, 74). Elytral striae shallowly engraved, intervals rather flat. In all other characters as described for the new genus, above.

Female genitalia: Length of apical gonocoxite about 0.15 mm; shape see Figs 76, 77; bursa copulatrix is not preserved. In all other characters as described for the new genus, above.

**Differential diagnosis.** *Quasicalathus agonicollis* sp. nov. differs from *Q. elpis* and *Q. conservans* sp. nov. by the smaller body ( $SBL < 7$  mm), more obtuse laterobasal angles of the pronotum, less concave elytral basal margin, less projected humeri, a more obtuse humeral angle ( $> 120^\circ$ ) and relatively smaller aedeagus. Based on specimen GZG 16188, *Q. agonicollis* sp. nov. differs from *Q. elpis* and *Q. conservans* sp. nov. additionally by presence of moderately large isodiametric sculpticells on head disc (small and transverse meshes in *Q. elpis* and *Q. conservans* sp. nov.) and (from *Q. elpis*) by the smaller apical gonocoxite (unknown in *Q. conservans* sp. nov.). Due to the uncertainties in the identification of the *Q. agonicollis* sp. nov. non-type female specimen (see Remarks above), the latter differential characters need confirmation based on additional material. The eyes of the *Q. agonicollis* sp. nov. holotype and the GZG 16188 specimen are found to be proportionally smaller [ $EyL/HW(-) = 0.62$  resp.  $0.65$ ] than in *Q. elpis* ( $0.72$ ) and the *Q. conservans* sp. nov. holotype ( $0.72$ ).

***Quasicalathus conservans* Schmidt & Will, sp. nov.**

<http://zoobank.org/1EAF9667-E896-445B-ADED-0DA2B055DF2B>

**Material studied.** Male in Rovno amber, with specimen label data “SDEI-Amb-002529”, deposited in the Senckenberg Deutsches Entomologisches Institut, Müncheberg, Germany. Size of the amber piece  $20 \times 10 \times 8.5$  mm.

Preservation status: The amber is clear but pervaded by numerous small air bubbles and extensive flowlines attached to the embedded fossil that is therefore only partly visible using light microscopy (Figs 32, 33). The exoskeleton of the fossil, including most parts of the aedeagus, is well preserved and, therefore, important diagnostic characters could be reconstructed using micro-CT (Figs 78–89).

Syninclusions: One stellate hair, few tiny dust particles.

**Description.** Measurements see Table 2.

Standardized body length: 7.3 mm.

Proportions:  $A3L/HL = 0.44$ ;

$EyL/HW(-) = 0.72$ ;

$PW/HW(+) = 1.40$ ;

$PW/PL = 1.27$ ;

$PW/PWb = 1.11$ ;

$PWb/PWa = 1.46$ ;

$EW/PW = 1.64$ ;

$EL/EW = 1.51$ ;

$EpL/EpW = 1.43$ ;

$EL/FL = 2.58$ ;

$EL/AedL = 3.64$ .

Head: As described in *Q. elpis*.

Prothorax: Pronotal lateral margin moderately narrowed toward base, slightly concave before laterobasal angles, angles slightly obtuse (Fig. 78). Prosternal process with traces of a lateral bead (Fig. 85). In all other characters as described for the new genus, above.

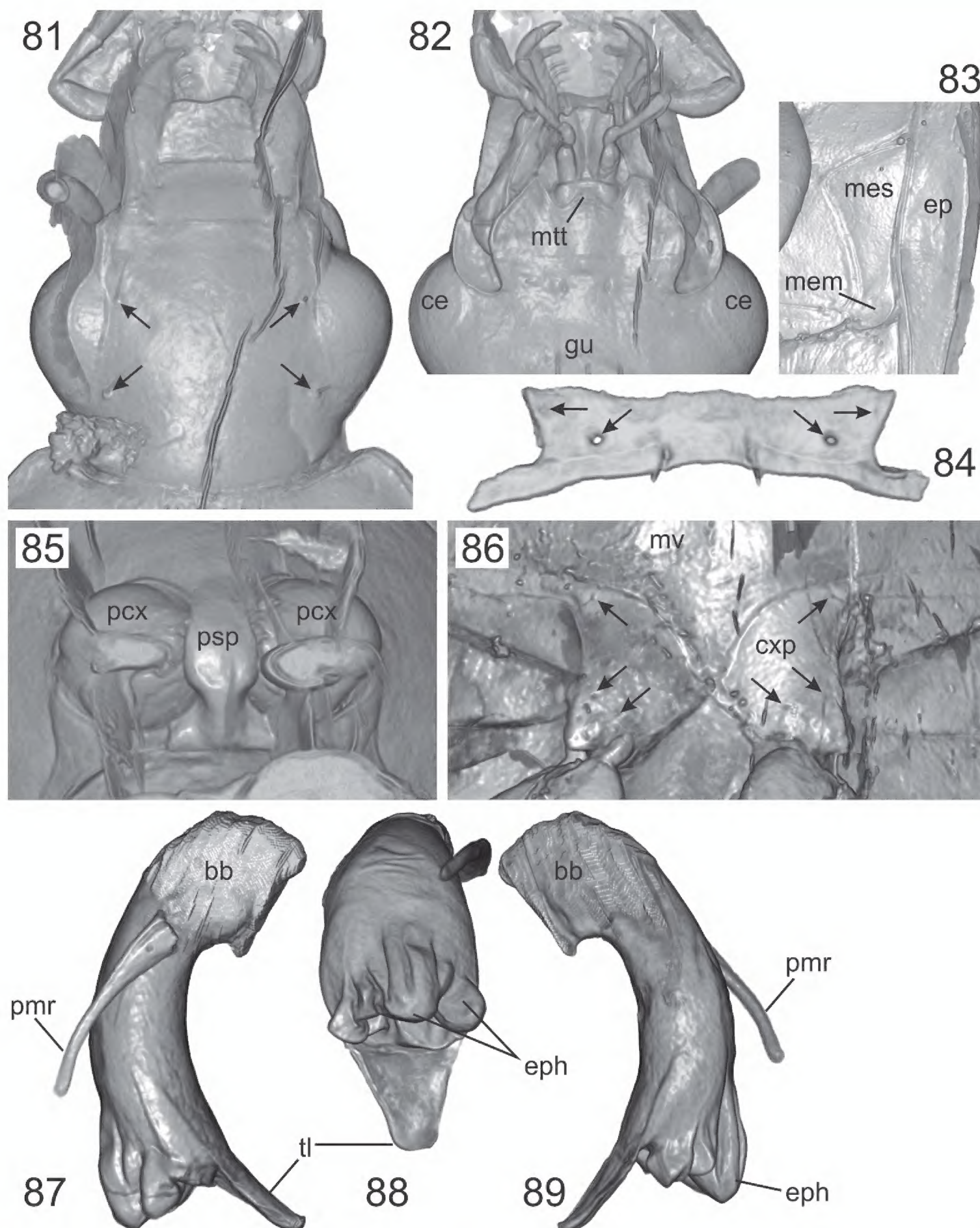
Pterothorax: Elytra with basal margin markedly concave and humerus markedly protruded anteriorly; basal margin forming a slightly obtuse angle (ca.  $115^\circ$ ) with the lateral margin (Fig. 78). Elytral striae moderately deeply engraved, intervals moderately convex. In all other characters as described for the new genus, above.

Aedeagus: Length of median lobe about 1.33 mm; median lobe terminal lamella moderately long, almost evenly narrowed from base to apex (Fig. 88); terminal lamella almost straight, with tip very slightly bent ventrally (Figs 87, 89). In all other characters as described for the new genus, above.

**Differential diagnosis.** In external characters, *Q. conservans* sp. nov. appears identical to *Q. elpis*, however, it can be distinguished by the male genitalia. The new species differs by the proportionally larger aedeagus ( $EL/AedL = 3.64$  instead of  $4.05$  in *Q. elpis*) and by the shape of the median lobe terminal lamella that is nearly evenly narrowed toward the apex if viewed in dorsal aspect and almost straight if viewed laterally (Figs 43, 44 versus 87, 89). *Quasicalathus conservans* sp. nov. differs from the above-described *Q. agonicollis* sp. nov. by larger body ( $SBL > 7$  mm), less obtuse laterobasal pronotal angles, the more markedly concave elytral basal margin, more markedly projected humeri, the less obtuse humeral angle ( $< 120^\circ$ ), and by the larger aedeagus.

**Remarks.** *Quasicalathus conservans* sp. nov. and *Q. elpis* are, based on current knowledge,





**Figures 81–89.** *Quasicalathus conservans* sp. nov., volume rendering of the holotype. **81.** Head, dorsal aspect (the arrows point to the insertions of the supraorbital setae); **82.** Head, ventral aspect; **83.** Left external part of metathorax, ventral view; **84.** Submentum (the arrows point to the insertions of the four lateral setae); **85.** Posterior part of prosternum and procoxae; **86.** Posterior part of metasternum and metacoxae; **87–89.** Preserved remains of the aedeagus (**87.** Right lateral aspect; **88.** Dorsal aspect; **89.** Left lateral aspect). Abbreviations: **bb** – basal bulb of aedeagal median lobe; **ce** – compound eye; **cxp** – metacoxal plate; **eph** – partly evaginated lobes of endophallus; **gu** – gula; **mem** – metepimeron; **mes** – metepisternum; **mtt** – mentum tooth; **mv** – metaventricle; **pcx** – procoxa; **pmr** – preserved distal part of right paramere of aedeagal median lobe; **psp** – prosternal process; **sc** – scutellum; **sps** – setae of sensory pit; **tl** – terminal lamella of aedeagal median lobe.

indistinguishable in their external characters but differ clearly in the shape and proportions of the male genitalia. Ball and Nègre (1972) and Schmidt (2018) detailed a similar situation found among many species pairs of Mexican and Himalayan *Calathus* that can only be separated by features of the male genitalia. We hypothesize that *Q. elpis* and *Q. conservans* sp. nov. were most likely allopatric species, distributed in geographically separated parts of the Eocene amber

forests of northern Europe. Under this hypothesis, *Q. elpis* was endemic to the more western part of the Eocene forest and was thus fossilized in Baltic amber, while *Q. conservans* sp. nov. was endemic to the more eastern part of the area and therefore fossilized in Rovno amber. This assumption is consistent with the faunistic data showing that beetle fossils of Baltic and Rovno amber deposits have only few species in common (less than 13%; Matalin et al. 2021).



## Conclusions

Sphodrine beetles were present in the Eocene amber producing forest with at least one genus (*Quasicalathus* gen. nov.) including three closely related species that we have identified from Baltic and Rovno amber deposits. However, the presence of the genus *Calathus* and subtribe Calathina in the Eocene forests of Central Europe, as was hypothesized by previous authors, was not substantiated as we found no evidence for this. The systematic limits of our result are due to the fact that apomorphic morphological characters defining Calathina and *Calathus* remain unknown (Schmidt and Will 2020). We propose the new taxon *Quasicalathus* gen. nov. for the *Calathus*-like fossil beetles from Baltic and Rovno amber and place this genus within the “P clade” of Sphodrini (Ruiz et al. 2009), which includes all sphodrine except Atranopsina, but without further affiliation to any of the subtribes. *Quasicalathus* may or may not be a member of Calathina, but it is not representative of Dolichiina, Pristosiina, Sphodrini, or Synuchina due to the absence of their respective group-specific derived characters. As such, *Quasicalathus* could be placed as sister to or a stem-group of any of these subtribes. In order to solve the problem of uncertain taxonomic position of this fossil species group a comprehensive phylogenetic analysis of recent and fossil sphodrine beetles is needed that combines morphological and molecular data in order to present a new basis for understanding character evolution in this group.

In addition to the open question of species-group taxonomy, verifying the true identity and full set of character states of *C. elpis* remains a task for future studies. In the present study, we could not solve this problem simply due to the unavailability of the holotype. Given that *C. elpis* is reported to have two anomalous character states for elytral and metacoxal chaetotaxy as described by Ortuño and Arillo (2009) there is a slight possibility that it represents a fourth fossil species that is not represented in our current material. However, we believe that both the concerning character states—5<sup>th</sup> elytral interval setose and external posterior seta of metacoxa absent—are simply erroneously attributed to *C. elpis*. This may be resolved when study of the holotype is possible. While the situation is unfortunate at present, our study does show the impact on taxonomic and systematic studies when nomenclatural type specimens are not made available to the scientific community as recommended in The Code (ICZN 1999, Recommendation 72F).

Given that 12 fossil specimens of *Quasicalathus* are now known from Eocene amber deposits, it appears that these beetles were a characteristic element of the amber producing forests of that period. Insect and plant evidence suggests that these amber producing forests grew under warm and humid climatic conditions (Kohlman-Adamska 2001, Alekseev and Alekseev 2016, Sadowski et al. 2017). Taken together, this suggests that the habitat preferences of *Quasicalathus* species were probably like that of the extant Canarian *Lauricalathus* Machado and *Trichocalathus* Bolívar y Pielain, and the Himalayan *Spinocalathus*

Schmidt. All groups with species adapted to warm, humid forest in the cloud-forest zone of high mountains in lower latitudes (Machado 1992, Schmidt 2018).

Many carabid beetles have denticulate or pectinate tarsal claws including *Abaris* Dejean (Pterostichini), many genera of Lebiini, Cyclosomini, Platynini, and Sphodrini. Denticulate claws probably provide greater grip for movement on irregular and vertical surfaces (Stork 1987) and have been proposed as one of the morphological adaptations to an arboricolous way of life (Erwin 1979, 1985). However, an evolutionary association of pectinate claws and arboreality has been shown to be ambiguous (Ober 2003). Even though there may not be a significant correlation between claw pectination and a fully arboricolous life history, there does seem to be a general tendency for species with pectinate claws to be found in sandy or loose soil habitats if geophilic (e.g., Cyclosomini and *Abaris*) or if more eurytopic, then frequently climbing trunks, rocky cliffs, and herbaceous plants, especially at night, or sheltering under bark (Baehr 1990) during the day. Frequent climbing behaviour would provide an explanation as to how presumably terrestrial beetles that show no evidence of flying at the time of inclusion may have been trapped in tree resin flows in the relatively high numbers observed in *Quasicalathus*. The denticulate tarsal claws found in many sphodrine are considered an apomorphic feature within Sphodrini (Casale 1988) and is proposed as a synapomorphy for the ‘P clade’ of Ruiz et al. (2009). It is possible that the Eocene *Quasicalathus* species represent a group of the ‘P clade’ characterized by propensity to climb, as is known for some extant *Calathus*, *Laemostenus* and *Pristonychus* species (Casale, pers. comm. 2022).

## Acknowledgements

We are very grateful to Alexander Gehler (Geoscientific Centre and Museum of the Georg-August-University, Göttingen), Carsten Gröhn (Glinde), and Christel and Hans Werner Hoffeins (Hamburg) for providing amber inclusions for the present study. We thank Achille Casale and Jim Liebherr for their valuable comments that helped us improve the manuscript. The study of JS was supported by the German Research Council (DFG grant SCHM 3005/3-2). The micro-CT machine used at the Rostock University to study the fossil specimens was jointly sponsored by the German Research Council and the country of Mecklenburg-Vorpommern (DFG INST 264/130-1 FUGG).

## References

- Alekseev VI, Alekseev PI (2016) New Approaches for Reconstruction of the Ecosystem of an Eocene Amber Forest. *Biology Bulletin* 43: 75–86. <https://doi.org/10.1134/S1062359016010027>
- Bachofen-Echt A (1949) *Der Bernstein und seine Einschlüsse*. Wunderlich Verlag, Straubenhardt, 230 pp. [Reprint 1996] [https://doi.org/10.1007/978-3-7091-2303-4\\_2](https://doi.org/10.1007/978-3-7091-2303-4_2)



- Baehr M (1990) The carabid community living under the bark of Australian eucalypts. In: Stork NE (Ed.) The role of ground beetles in ecological and environmental studies. Intercept, Andover, 3–11.
- Ball GE, Nègre J (1972) The taxonomy of the Nearctic species of the genus *Calathus* Bonelli (Coleoptera: Carabidae: Agonini). Transactions of the American Entomological Society 98: 412–533.
- Bousquet Y (2012) Catalogue of Geadephaga (Coleoptera, Adephaga) of America north of Mexico. Sphodrini – Pseudomorphini. ZooKeys 245(3): 1161–1722. <https://doi.org/10.3897/zookeys.245.3416>
- Casale A (1988) Revisione degli Sphodrini (Coleoptera, Carabidae, Sphodrini). Museo Regionale di Scienze Naturali, Torino, 1024 pp.
- Gomez RA, Will KW, Maddison DR (2016) Are *Miquihuanarhadiniiformis* Barr, 1982 and *Pseudamara arenaria* (LeConte, 1847) (Coleoptera, Carabidae) sphodrine? Phylogenetic analysis of data from next-generation sequencing of museum specimens resolves the tribal-group relationships of these enigmatic taxa. Entomologische Blätter und Coleoptera 112: 149–168.
- Erwin TL (1979) Thoughts on the evolutionary history of ground beetles: hypotheses generated from comparative faunal analyses of lowland forest sites in temperate and tropical regions. In: Erwin TL, Ball GE, Whitehead DR, Halpern AL (Eds) Carabid beetles: their evolution, natural history, and classification. Dr W. Junk, The Hague, 539–592. [https://doi.org/10.1007/978-94-009-9628-1\\_30](https://doi.org/10.1007/978-94-009-9628-1_30)
- Erwin TL (1985) The taxon pulse: a general pattern of lineage radiation and extinction among carabid beetles. In: Ball GE (Ed.) Taxonomy, phylogeny and zoogeography of beetles and ants. Dr W. Junk, Dordrecht, 437–472.
- Habu A (1978) Fauna Japonica. Carabidae: Platynini. Keigaku Publishing, Tokyo, 447 pp.
- Handlirsch A (1908) Die fossilen Insekten und die Phylogenie der rezenten Formen: Ein Handbuch für Paläontologen und Zoologen, Teil 1. Engelmann, Leipzig, [12 +] 1430 pp. <https://doi.org/10.5962/bhl.title.5636>
- Hoffeins C (2012) On Baltic amber inclusions treated in an autoclave. Polish Journal of Entomology 81: 165–181. <https://doi.org/10.2478/v10200-012-0005-z>
- Hovorka O (2017a) Subtribe Calathina Laporte, 1834. In: Löbl I, Löbl D (Eds) Catalogue of Palearctic Coleoptera, Volume 1. Second edition. Brill Publishers, Leiden, Boston, 760–768.
- Hovorka O (2017b) Subtribe Dolichina Brullé, 1834. In: Löbl I, Löbl D (Eds) Catalogue of Palearctic Coleoptera, Volume 1. Second edition. Brill Publishers, Leiden, Boston, 768–769.
- ICZN [International Commission on Zoological Nomenclature] (1999) International code of zoological nomenclature. 4<sup>th</sup> edn. International Trust for Zoological Nomenclature, c/o Natural History Museum, London, 306 pp. <https://doi.org/10.5962/bhl.title.50608>
- Jeannel R (1926) Monographie des Trechinae. Morphologie comparée et distribution géographique d'un groupe de Coléoptères (Première livraison). L'Abeille, Paris 32: 221–550.
- Klebs EHR (1910) Über Bernsteineinschlüsse im Allgemeinen und die Coleopteren meiner Bernsteinsammlung. Schriften der Königlich Physikalisch-ökonomischen Gesellschaft zu Königsberg i. Pr., 51: 217–242.
- Kohlman-Adamska A (2001) A graphic reconstruction of an „amber“ forest. In: Kosmowska-Ceranowicz B (Ed.) The amber treasure trove. Part I. The Tadeusz Giecwicz's collection at the Museum of the Earth, Polish Academy of Sciences, Warsaw, Documentary Studies 18: 15–18.
- Larsson SG (1978) Baltic amber – a palaeobiological study. Entomograph 1: 1–192.
- Lindroth CH (1956) A revision of the genus *Symachus* Gyllenhal (Coleoptera: Carabidae) in the widest sense, with notes on *Pristosia* Motschulsky (*Eucalathus* Bates) and *Calathus* Bonelli. The Transactions of the Royal Entomological Society of London 108: 485–576. <https://doi.org/10.1111/j.1365-2311.1956.tb01274.x>
- Machado A (1992) Monografía de los carábidos de las Islas Canarias. Instituto de Estudios Canarios, La Laguna, 734 pp.
- Matalin AV, Perkovsky EE, Vasilenko DV (2021) First record of tiger beetles (Coleoptera: Cicindelidae) from Rovno amber, with the description of a new genus and species. Zootaxa 5016(2): 243–256. <https://doi.org/10.11646/zootaxa.5016.2.5>
- Ober K (2003) Arboreality and morphological evolution in ground beetles (Carabidae: Harpalinae): testing the taxon pulse model. Evolution 57(6): 1343–1358. <https://doi.org/10.1111/j.0014-3820.2003.tb00342.x>
- Ober K, Heider TN (2010) Phylogenetic diversification patterns and divergence times in ground beetles (Coleoptera: Carabidae: Harpalinae). BMC Evolutionary Biology 10: e262. <https://doi.org/10.1186/1471-2148-10-262>
- Ortuño VM, Arillo A (2009) Fossil carabids from Baltic amber – A new species of the genus *Calathus* Bonelli, 1810 (Coleoptera: Carabidae: Pterostichinae). Zootaxa 2239: 55–61. <https://doi.org/10.11646/zootaxa.2239.1.5>
- Ruiz C, Jordal B, Serrano J (2009) Molecular phylogeny of the tribe Sphodrini (Coleoptera: Carabidae) based on mitochondrial and nuclear markers. Molecular Phylogenetics and Evolution 50(1): 59–73. <https://doi.org/10.1016/j.ympev.2008.09.023>
- Ruiz C, Jordal BH, Emerson BC, Will KW, Serrano J (2010) Molecular phylogeny and Holarctic diversification of the subtribe Calathina (Coleoptera: Carabidae: Sphodrini). Molecular Phylogenetics and Evolution 55: 358–371. <https://doi.org/10.1016/j.ympev.2009.10.026>
- Ruiz C, Jordal BH, Serrano J (2012) Diversification of subgenus *Calathus* (Coleoptera: Carabidae) in the Mediterranean region – glacial refugia and taxon pulses. Journal of Biogeography 39(10): 1791–1805. <https://doi.org/10.1111/j.1365-2699.2012.02751.x>
- Sadowski E-M, Schmidt AR, Seyfullah LJ, Kunzmann L (2017) Conifers of the ‘Baltic Amber Forest’ and their palaeoecological significance. Stapfia 106: 1–73.
- Schmidt J (2018) Notes on the taxonomy of *Calathus* Bonelli, 1810, with special reference to the *C. heinertzi* group from the Nepal Himalaya (Insecta: Coleoptera: Carabidae: Sphodrini). In: Hartmann M, Barclay MVL, Weipert J (Eds) Biodiversity and Natural Heritage of the Himalaya. Vol. VI. Verein der Freunde und Förderer des Naturkundemuseums Erfurt e.V., Erfurt, 297–318.
- Schmidt J, Belousov I, Michalik P (2016) X-Ray microscopy reveals endophallic structures in a new species of the ground beetle genus *Trechus* Clairville, 1806 from Baltic amber (Coleoptera: Carabidae: Trechini). ZooKeys 614: 113–127. <https://doi.org/10.3897/zookeys.614.9283>
- Schmidt J, Michalik P (2017) The ground beetle genus *Bembidion* Latreille in Baltic amber: Review of preserved specimen and first 3D reconstruction of endophallic structures using X-ray microscopy (Coleoptera: Carabidae: Bembidiini). ZooKeys 662: 101–126. <https://doi.org/10.3897/zookeys.662.12124>
- Schmidt J, Scholz S, Kavanaugh DH (2019) Unexpected findings in the Eocene Baltic amber forests: Ground beetle fossils of the tribe Nebriini (Coleoptera: Carabidae). Zootaxa 4544(1): 103–112. <https://doi.org/10.11646/zootaxa.4701.4.2>



- Schmidt J, Scholz S, Maddison DR (2021) *Balticeler kerneggeri* gen. nov., sp. nov., an enigmatic Baltic amber fossil of the ground beetle subfamily Trechinae (Coleoptera, Carabidae). – Deutsche Entomologische Zeitschrift 68(1): 207–224. <https://doi.org/10.3897/dez.68.66181>
- Schmidt J, Will K (2020) A new subgenus for “*Acalathus*” *advena* (LeConte, 1846) and the challenge of defining Calathina based on morphological characters (Coleoptera, Carabidae, Sphodrini). Zootaxa 4544(4): 581–588. <https://doi.org/10.11646/zootaxa.4722.4.2>
- Sciaky R, Facchini S (1997) *Xestopus cyaneus* new species from China (Coleoptera Carabidae). Bolletino della Società Entomologica Italiana 129(3): 235–240.
- Sciaky R, Wrase DW (1998) Two new genera of Sphodrini Dolichina from China (Coleoptera Carabidae). Bolletino della Società Entomologica Italiana 130(3): 221–232.
- Spahr U (1981) Systematischer Katalog der Bernstein- und Kopal-Käfer (Coleoptera). Stuttgarter Beiträge zur Naturkunde, Serie B, 80: 1–107.
- Standke H (2008) Bitterfelder Bernstein gleich Baltischer Bernstein? – Eine geologische Raum – Zeit – Betrachtung und genetische Schlußfolgerungen. Exkursionsführer und Veröffentlichungen der Deutschen Gesellschaft für Geowissenschaften 236: 11–33.
- Stork N (1987) Adaptations of arboreal carabids to life in trees. Acta Phytopathologica et Entomologica Hungarica 22: 273–291.
-